

Exploring Gripping Behaviours and Haptic Emotions for Human-Robot Handshaking

Erforschung von Greifverhalten und haptischen Emotionen für Mensch-Roboter-Handshake

Master thesis by Zhicheng Yang

Date of submission: 10. February 2022

1. Review: Prof. Dr. Jan Peters
2. Review: Prof. Dr. Heinz Koepl
3. Review: Prof. Dr. Dr. Ruth Stock-Homburg
4. Review: M.Sc. Vignesh Prasad
Darmstadt



TECHNISCHE
UNIVERSITÄT
DARMSTADT



Erklärung zur Abschlussarbeit gemäß §22 Abs. 7 und §23 Abs. 7 APB der TU Darmstadt

Hiermit versichere ich, Zhicheng Yang, die vorliegende Masterarbeit ohne Hilfe Dritter und nur mit den angegebenen Quellen und Hilfsmitteln angefertigt zu haben. Alle Stellen, die Quellen entnommen wurden, sind als solche kenntlich gemacht worden. Diese Arbeit hat in gleicher oder ähnlicher Form noch keiner Prüfungsbehörde vorgelegen.

Mir ist bekannt, dass im Fall eines Plagiats (§38 Abs. 2 APB) ein Täuschungsversuch vorliegt, der dazu führt, dass die Arbeit mit 5,0 bewertet und damit ein Prüfungsversuch verbraucht wird. Abschlussarbeiten dürfen nur einmal wiederholt werden.

Bei der abgegebenen Thesis stimmen die schriftliche und die zur Archivierung eingereichte elektronische Fassung gemäß §23 Abs. 7 APB überein.

Bei einer Thesis des Fachbereichs Architektur entspricht die eingereichte elektronische Fassung dem vorgestellten Modell und den vorgelegten Plänen.

Darmstadt, 10. February 2022

zhicheng yang

Z. Yang

Abstract

The handshake is very popular as a universal greeting in social situations. The handshake as a physical interaction can convey emotions to a certain extent. For example, handshake behaviour when humans are nervous is not the same as when they are sad. Therefore, handshaking is a valuable behavior to research in the context of Human-Robot Handshaking to make a robot seem more natural and acceptable to humans. For doing so, we need to be able to control the robot grip force interactively. A comfortable grip force in Human-Robot Handshaking can improve the human impression of the robot. In this thesis, we explore behaviours for Human-Robot Handshaking by using a more principled model, namely the Force-Impedance model, to control the robot grip force and behaviour. In our experiments, we extend existing approaches, where the robot grip force was estimated with the measured human grip force, and there was no control for the robot grip force. However, in our experiments, the human grip force and the robot grip force can be measured. Therefore, we can implement control for the measured robot grip force in this case. Our proposed model can adjust the robot grasp to give a comfortable handshake in Human-Robot Handshaking. The results show that the proposed model in Human-Robot Handshaking thereby enables an interactive synchronization between a human and a robot.

Zusammenfassung

Das Händeschütteln ist als universelle Begrüßung in sozialen Situationen sehr beliebt. Das Händeschütteln als physische Interaktion kann bis zu einem gewissen Grad Emotionen vermitteln. Zum Beispiel ist das Verhalten beim Händeschütteln, wenn Menschen nervös sind, nicht dasselbe wie wenn sie traurig sind. Daher ist das Händeschütteln ein wertvolles Verhalten, das im Zusammenhang mit dem Mensch-Roboter-Handshake erforscht werden sollte, um einen Roboter natürlicher und akzeptabler für Menschen erscheinen zu lassen. Dazu müssen wir in der Lage sein, die Greifkraft des Roboters interaktiv zu steuern. Eine angenehme Griffkraft beim Mensch-Roboter-Handshake kann den menschlichen Eindruck des Roboters verbessern. In dieser Arbeit erforschen wir Verhaltensweisen für das Mensch-Roboter-Handshake, indem wir ein prinzipielleres Modell, nämlich das Kraft-Impedanz-Modell, zur Steuerung der Robotergriffkraft und des Verhaltens verwenden. In unseren Experimenten erweitern wir bestehende Ansätze, bei denen die Greifkraft des Roboters anhand der gemessenen menschlichen Greifkraft geschätzt wurde und es keine Kontrolle für die Greifkraft des Roboters gab. In unseren Experimenten können jedoch die menschliche Griffkraft und die Robotergriffkraft gemessen werden. Daher können wir in diesem Fall eine Steuerung für die gemessene Robotergriffkraft implementieren. Unser vorgeschlagenes Modell kann den Robotergriff so anpassen, dass ein komfortabler Händedruck beim Mensch-Roboter-Handshake entsteht. Die Ergebnisse zeigen, dass das vorgeschlagene Modell im Mensch-Roboter-Handshake eine interaktive Synchronisation zwischen Mensch und Roboter ermöglicht.

Contents

1. Introduction	2
1.1. Main Contributions	3
1.2. Outline	3
2. Related Work	5
3. Foundations and Methods	8
3.1. Foundations	8
3.1.1. Impedance and Admittance models	8
3.1.2. PID Control	11
3.2. Force Sensing for Handshaking	13
3.3. Proposed Methods	15
4. Experiments and Results	18
4.1. Experiment Setups	18
4.1.1. Hardware Setup	18
4.1.2. Software Setup	20
4.2. Force Sensing Grid Calibration	24
4.3. Baseline Interactive Handshaking Behaviour	29
4.4. Improved interactive Handshaking Behavior	31
5. Summary and Future Work	40
5.1. Summary	40
5.2. Future Work	41
A. Appendix	47
A.1. Topic Connection	47
A.2. Parameters Turning	48

1. Introduction

Humans always perform handshaking as a sign of greeting when they first meet. The handshake is an embodied interaction through physical contact, by which humans can synchronize their embodied rhythms directly. The synchronization of embodied rhythms promotes the sharing embodiment. It is considered that humans construct a relationship that is emotionally acceptable to each other by the synchronization of the embodied rhythms and sharing embodiment [1]. Socially, a comfortable handshake symbolizes acceptance and respect for others so that one can be able to make an excellent initial impression, which may lead to future cooperation and coexistence [2].

Suppose a robot generates a handshake motion that is emotionally acceptable to humans. In that case, it will lessen any feeling of aversion that the human has when initiating an interaction with the robot, which makes humans more willing to get along with robots [3]. In particular, robots are expected to play an essential role in social welfare and service for older citizens, one of the critical applications of HRI (Human-Robot Interaction).

What makes handshaking a more critical interaction than other interactions is precisely the importance of the touch in HRI. At the beginning of life, the importance of nonverbal communication, particularly tactile stimulation, supersedes verbal communication. Even before the child's first word is spoken, the groundwork for verbal communication has been laid by touch and other modalities of nonverbal communication [4]. Understanding the possibilities and mechanisms, by which practical touch can operate, has implications for the design of many HRI applications, ranging from fostering companionship to therapeutic interventions for children, the ill, and the elderly [5].

Although there is considerable work on the Human-Robot Handshaking research, there are still some pitfalls in the current state. Currently, most works do not implement proper grip control, which is crucial for capturing the expressive ability of handshakes to its maximum. Additionally, the human-likeness of an interface is just as crucial as its perception. Even a robot hand with sophisticated mechanisms, like the Android robot used in [6], which has a soft skin-like layer and heated palms, is still easily distinguished from a human

hand. Thus, developing better social robot interfaces that have a proper force sensing mechanism and can perform reasonable closed-loop control will be more important for a robot [7].

1.1. Main Contributions

In this thesis, we use the BionicSoftHand to investigate the gripping behavior in Human-Robot Handshaking. We develop a control model called the Force-Impedance model for the BionicSoftHand to control its gripping behaviour and force in Human-Robot Handshaking. By our control model, the BionicSoftHand can sense the grip force exerted by the human hand and accordingly adjust its grip force and motion (opening or closing) in Human-Robot Handshaking.

It is an essential aspect of handshaking since the handshake can convey emotions, e.g., tension and excitement. Therefore, a robot hand needs to give a suitable grip force and respond adequately in a synchronous manner in Human-Robot Handshaking, increasing the human impression for the robot and thus facilitating HRI. In addition, human emotions also can be sensed according to the human grip force in Human-Robot Handshaking. Therefore, in our future work, the BionicSoftHand will attempt to detect haptic emotions by the grip force exerted by the human hand based on our control model.

1.2. Outline

The construction of this thesis is shown in the following paragraphs.

Chapter 1 describes the background and importance of Human-Robot Handshaking in HRI. Moreover, we illustrate the main contributions of this thesis. Finally, we give an outline of this thesis.

Chapter 2 introduces an overview of related work on Human-Robot Handshaking and gives an extended work in this thesis.

Chapter 3 introduces the relative foundations to research Human-Robot Handshaking and proposes our control model for Human-Robot Handshaking based on these foundations.

Chapter 4 describes our experiments. Then, we implement the handshaking experiments, obtain the results, and finally evaluate our experiments.



Chapter 5 summarizes our work in this thesis. The contributions and shortcomings of our work are discussed. In addition, we give an outlook about future work.

2. Related Work

This chapter discusses related work on Human-Robot Handshaking, which guided and inspired our work in this thesis. Moreover, we present our extended work based on these previous works. We mainly cover the works from [8] and a more detailed overview of Human-Robot Handshaking can be found in [9] and [7].

Tagne et al. [10] studied and analyzed the physical parameters of the handshake to use its characteristic features (frequency, duration, strength, synchronization) to model this interaction. Moreover, in [11] a new wearable sensor network to measure a handshake was described. It consists of sensors attached to the glove and a micro-controller for signal acquisition and conditioning. The proposed system allowed reproducible experiments to quantify handshake characteristics such as duration, strength, vigor, and rhythmicity.

In [1] a handshake robot system for embodied interaction was developed. The robot can generate the handshake approaching motion acceptable to humans by using secondary delay elements from the trajectory of a human hand. Moreover, Jindai et al. [12] analyzed this handshake approaching motion in cases with and without voice greeting and proposed a handshake approaching motion model based on the analysis. Furthermore, in [13] a shake-motion leading model was proposed, which generated a leading motion to transit from approaching motion to shaking motion.

In [14] a hand position recognition method was proposed, in which a 3D model of a human arm was used. This method was adopted in the developed robot system to recognize the position of a human hand without requiring prior contact or any restrictions on humans. Moreover, Jindai et al. [12] proposed a handshake request motion model, with which a robot requests humans for a handshake. Furthermore, a handshake response motion model to generate a handshake approaching motion before actually shaking hands with the human was proposed in [15], where the robot responds to a handshake when the human requests a handshake. Furthermore, A switching handshake control is developed in [3], where the robot generates either the request motion or the response motion for a handshake according to the motion of the approaching human.

Knoop et al. [16] presented two benchmark experiments. In the first experiment, they measured the contact locations in Human-Human Handshaking. The second experiment measured the contact pressure distribution for handshakes with a sensorized palm. In addition, they performed the contact area test on the RBO Hand 2 [17], and the contact pressure distribution test on the Pisa/IIT SoftHand [18] to evaluate the "handshakiness" of these robot hands.

A handshake telephone system using robot hands was proposed in [19], through which two users can shake hands with each other while talking on the telephone. The proposed system can be used for telephone handshake communication and amusement and for telephone diagnosis in some kinds of diseases to develop a medical application of HMI (Human-Machine Interface). Furthermore, in [20], a communication system that allows two persons in different locations to shake hands was developed, and a novel haptic interface capable of performing a handshake was designed and built.

Arns et al. [21] presented a novel robot hand design that aimed at producing a realistic Human-Robot Handshaking. A standard characteristic model of human-palm compliance was developed based on human hand anatomy and an empirical study. This model implemented a realistic palm-compliance rendering, and a position-controlled feedback loop rendered human-like agility.

In [22] a novel scheme of modeling human haptic skill was proposed. The problem of motion synthesis and force-based impedance control were studied, and a switching model prototype with superposed output and force-based impedance control was obtained. The robot with this model was capable of handshaking realistically with a passive partner.

Orefice et al. [23] created a handshake model based on the tactile features activated during handshaking, which can discriminate intrinsic characteristics of a person such as gender or extroversion. The results showed that it is possible to recognize gender and extroversion personality traits based on the firmness and movement of handshaking. For instance, smaller pressure and frequency were found to describe female handshakes, and higher speed amplitude describes introverted handshakes.

Avelino et al. [24] developed a platform for exploring Human-Robot Handshaking. A state-of-the-art tactile sensor can accurately measure the force vector in real-time at each contact point. In order to research a confident and pleasant grasp based on tactile sensing, a handshake experiment was set up, where the subjects shake hands with Vizzy [25]. Three different grasping models, namely strong, medium, and weak grasp, corresponding to different degrees of the closing of the robot hand, were implemented. The results showed that female subjects preferred a slightly larger grip force than the male, and

there was more considerable variability, which the hand size of the participants may cause. In order to resolve this problem to obtain a pleasant grasp, an further study was carried out in [26]. In this study, the participants grasped the robot by themselves until a preferable grasp was reached. The robot's finger positions and the force measured by the sensors on the fingers were recorded in this process. Then two handshake experiments were implemented. In the first experiment, the robot hand grips participants' hands according to the previously recorded finger positions, namely a fixed handshake. In the second experiment, a force control handshake was implemented. The robot hand grips participants' hands according to the previously recorded force, which was regarded as the setpoint in a PID controller. Finally, participants evaluated the two handshakes and gave feedback.

Vigni et al. [8] proposed a closed-loop handshake control model in order to investigate Human-Robot Handshaking. A handshake experiment was implemented, where participants shook hands with the Pisa/IIT SoftHand [18] by mimicking its grasping force profile as it moved through a random closing sequence. In this process, the motion position of the robot hand was recorded, and the human grip force was measured and recorded. Thus, they obtained a relationship between the robot hand position and the human grip force. Furthermore, they estimated the robot grip force from the human grip force. They proposed three controllers based on the obtained relationship between the robot hand position and the human grip force: robot follower controller, robot open-loop controller, and combined controller. Participants evaluated the handshakes where the three controllers were used and gave feedback. Finally, they demonstrated that humans exploit closed-loop control for handshaking.

In this thesis, we expand the work on [26] and [8]. In [26] a PID controller was used to control the robot grip force, whose setpoint was a preferable grip force obtained from calibration experiments. However, this preferable grip force is a fixed force. Therefore, the interaction between the human hand and the robot hand was not taken into account. Moreover, in [8], the interaction between the human hand and the robot hand was considered. They control the closure of the robot hand based on the force exerted by a human. However, this fails to consider different hand sizes, which would change the force the robot exerts on the human.

Our work integrates the studies in [26] and [8]. We propose a handshake control model, which can control the robot motion and the robot grip force during Human-Robot Handshaking. The robot can implement a comfortable handshake with humans while maintaining the capability of HRI. The BionicSoftHand plays an important role in measuring both the human grip force and the robot grip force.

3. Foundations and Methods

This chapter introduces some foundations and methods in Human-Robot Handshaking research. Section 3.1 introduces the impedance and admittance models and PID control. Section 3.2 discusses force sensing and analyzes the contact area in Human-Robot Handshaking. Section 3.3 presents a handshake model applicable to our experiment, namely the Force-Impedance model.

3.1. Foundations

This section introduces the basic control models and methods. The impedance and admittance models are described in subsection 3.1.1, which are approaches to dynamic control relating to force and position. Then, in subsection 3.1.2, we present the PID control, which generally can be used as force control.

3.1.1. Impedance and Admittance models

Mechanical impedance reflects the relation between the driving force at the input to the body and the resultant movement of the body. If the human body is rigid, the ratio of force to acceleration applied to the body would be constant and indicate the subject's mass. However, because the body is not rigid, the ratio of force to acceleration is only close to the body mass at very low frequencies (below about 2 Hz with vertical vibration, below about 1 Hz with horizontal vibration) [27].

Before understanding the impedance and admittance controls, we first need to understand the position control. Suppose we have a spring whose stiffness is K_s , we now want to control the position of the spring from x to x_d , x is its actual position, and x_d is its desired

position. We add feedback and use a P controller will do the trick, as shown in Figure 3.1. This typical position control method precisely controls the position from x to x_d .

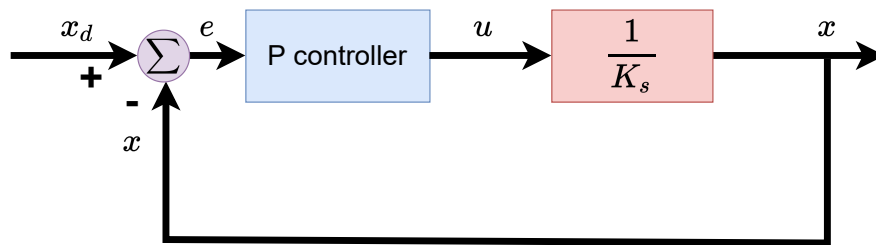


Figure 3.1.: Position control. x_d is the desired position, x is the actual position, e is the error between x_d and x , u is the control variable, K_s is the spring stiffness.

Now consider a situation where an external force F_{ext} is suddenly applied during the spring motion, which is a very unfriendly disturbance for the position controller, and this external force will cause the spring to shift. After the controller gets the feedback signal, the control output has the effect of suppressing the disturbance, and it breaks back the displacement that should have been shifted with more muscular control. A confrontation relationship is formed.

It can be seen that the position control is inherently repulsive to external forces, which can go wrong when the position accuracy demand is high and the environment is very stiff. On the other hand, once the position deviates and the environment is very stiff, a great force will be generated as the robot also has high stiffness, which will bring significant damage to the robot.

So we need a "soft" control. Let us imagine such a situation. The robot is moving, and if suddenly comes an external force, the robot will follow the external force to move. After the withdrawal of the external force, the robot then returns to the previous state. Like a person suddenly is pushed, he will produce an inertial movement.

So for spring with an external force, we design a control model to make it "soft", as shown in Figure 3.2.

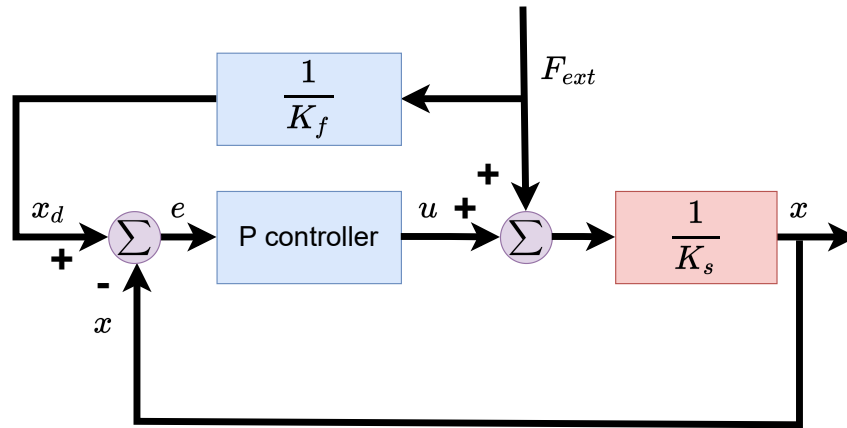


Figure 3.2.: "Soft" control. x_d is the desired position, x is the actual position. e is the error between x_d and x , u is the control variable. K_s is the spring stiffness, F_{ext} is the external force. K_f is control parameter.

According to this model, we can give the following equations,

$$(x_d - x)K + F_{ext} = K_s x, \quad (3.1)$$

$$K_f x_d = F_{ext}, \quad (3.2)$$

where K is the proportional gain of the P controller. Inserting Equation 3.2 to Equation 3.1 and eliminating x_d , the following equation between F_{ext} and x is given,

$$F_{ext} = K_f \frac{K_s + K}{K_f + K} x. \quad (3.3)$$

When the proportional gain is vast, the kinetic equation of the spring is approximated by the following form,

$$F_{ext} = K_f x. \quad (3.4)$$

The spring's displacement will follow the change of the external force in this case, the larger the external force, the larger the displacement of the spring, and the smaller the external force, the smaller the displacement of the spring. Moreover, by adjusting the magnitude of K_f , the stiffness characteristics of the spring can be changed. This control strategy is very friendly and quite "soft" for the spring, and when the external force is large, the spring conforms to it rather than fighting against it.

Equation 3.4 is an admittance control. When a robot is subjected to an external force, it will be shifted in its original trajectory to comply with the external force. The control goal is achieved with the internal position closed-loop controller by generating a new desired position according to the admittance controller.

The admittance control with a more general second-order equation has the following form,

$$M(\ddot{x}_d - \ddot{x}_0) + K(x_d - x_0) + D(\dot{x}_d - \dot{x}_0) = F_{ext}, \quad (3.5)$$

Let $e = x_d - x$, the following equation is given [28],

$$M\ddot{e} + D\dot{e} + Ke = F_{ext}. \quad (3.6)$$

where the positive constants M , D , and K represent the desired inertia, damping, and stiffness, respectively. F_{ext} is the external force. x_d is desired position. x_0 is initial desired position, if there is no external force, then x_d is equal to x_0 . e is the displacement.

Equation 3.6 is the core of the admittance and impedance controls, whose control task is to maintain this relationship between the external force and the displacement, rather than to make the object displacement track the desired displacement as in position control. In the above spring example, we can change the stiffness characteristics of the spring by adjusting K_f , and here the dynamical properties of the robot are changed by adjusting M , D , and K .

The core idea of the impedance control is the same as that of the admittance control, which is to ensure the relationship between the external force and the position error. The one different thing is that the admittance model defines the motion that results from a force, and the impedance control, which defines the force that results from a motion, is the inverse of admittance.

3.1.2. PID Control

In the process control, the PID controller is one of the most widely used automatic controllers, which can control the output signals by the terms of proportional (P), integral (I) and deviation (D). Therefore, the PID controller is an optimal control.

In order to achieve PID control, the system must be required to have feedback because it is a closed-loop control. An error is controlled according to the feedback to ensure the system's stability. As shown in Figure 3.3, the PID controller calculates a error $e(t)$ by comparing the reference input $r(t)$ with the actual output $y(t)$. The three terms of

the controller (P, I, D) control the error according to their respective control laws and superimpose the control results to obtain a control variable $u(t)$, which is processed by the system and the system gives feedback. The feedback result continues to be compared with the reference input, thus forming a closed-loop control.

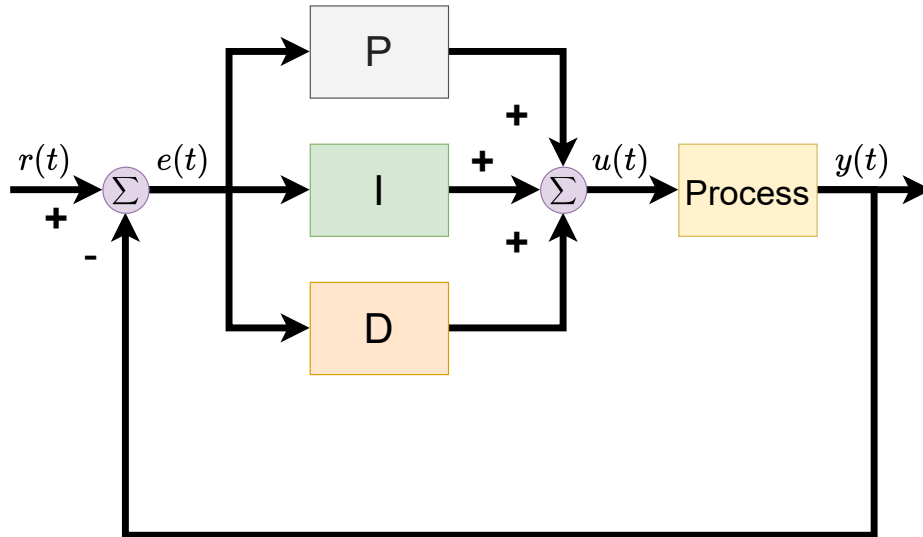


Figure 3.3.: PID controller. $r(t)$ is the reference input. $y(t)$ is the measured process output. $e(t)$ is the error between $r(t)$ and $y(t)$, $u(t)$ is the intermediate control variable.

The three terms of PID controller (P, I, D) have different control laws. P is a proportional control and has the following form,

$$P = K_p e(t), \quad (3.7)$$

where K_p is the proportional coefficient. Term P can faster overcome the effect of disturbances on the system, but only using a P controller can not make the system output stabilize at the desired value. There is a residual difference, namely steady-state error. This undesirable effect is particularly evident in the face of variable reference inputs.

Term I is an integral control and has the following control law,

$$I = K_i \int_0^t e(\tau) d\tau, \quad (3.8)$$

where K_i is an integral coefficient. Term I accounts for past values of the error and integrates them over time to eliminate the residuals based on a proportional control.

Term D is a derivative control and has the following form,

$$D = K_d \frac{de(t)}{dt}, \quad (3.9)$$

where K_d is a derivative coefficient. Term D better estimates the future trend, as it calculates a rate of change. Thus, it has an overriding effect. It can reduce the error effect by giving a control based on the rate of change. It has a significant effect on improving the dynamic performance of the system.

PID control is an ideal control law, and it introduces integration control based on proportional control to eliminate the residual difference. Moreover, derivative control is added to improve the stability of the system. PID control is the superposition of proportional, integral, derivative control effects. Its control law is given as the following form,

$$u(t) = K_p e(t) + K_i \int_0^t e(\tau) d\tau + K_d \frac{de(t)}{dt}. \quad (3.10)$$

Generally, PID control achieves the optimal control effect by adjusting the magnitude of three parameters K_p , K_i , and K_d . Nevertheless, sometimes we may only need to adjust one or two parameters to make the system perform well. For example, Controllers containing only two control parameters can be PI (Equation 3.11) or PD (Equation 3.12) controllers.

$$u(t) = K_p e(t) + K_i \int_0^t e(\tau) d\tau. \quad (3.11)$$

$$u(t) = K_p e(t) + K_d \frac{de(t)}{dt}. \quad (3.12)$$

Since the PID controller is a model-free control, adjusting the three parameters can vary greatly depending on the control object.

3.2. Force Sensing for Handshaking

This section introduces how the robot hand senses grip force through sensors. In particular, the human grip force and the robot grip force can be sensed differently by the

BionicSoftHand through sensors at different locations, so the distribution of sensors is crucial for the perception of grip force.

The contact area between the human hand and the robot hand is one of the factors that must be taken into account in the Human-Robot Handshaking, as it relates to the accurate measurement of the grip force. Knoop et al. [16] presented an experiment to measure the contact locations in Human-Human Handshaking with a sensorized palm. In this experiment, paint was applied to the hand of one participant. Then, a handshake was performed with a target participant, and the paint-transfer pattern on the hand of the target participant showed the contact area, as shown in Figure 3.4.

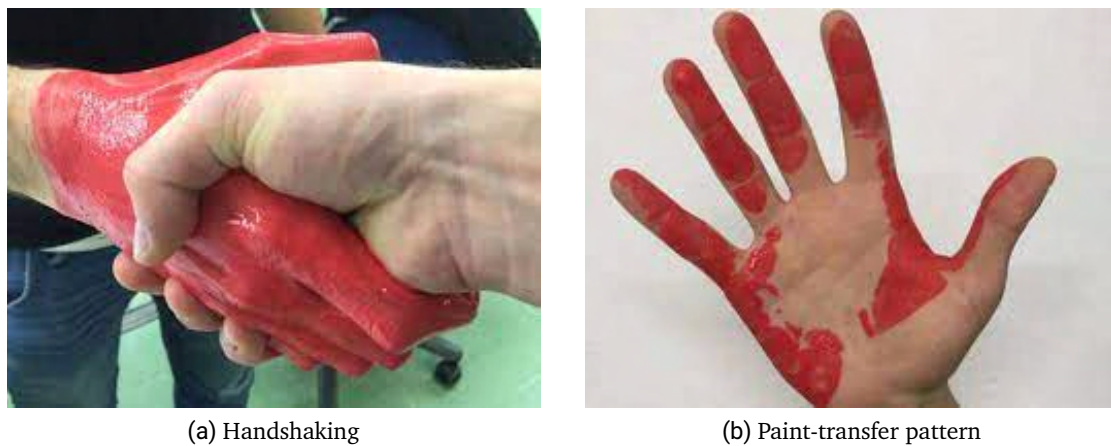
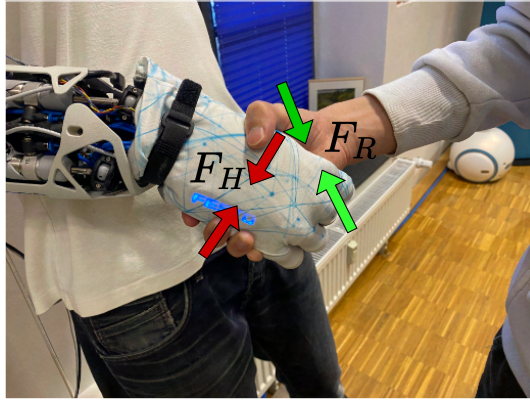


Figure 3.4.: Measuring contact area during handshaking [16]. (a) shows a handshake between two hands, the one is painted with red color, the other is clean. (b) shows how the paint is transferred.

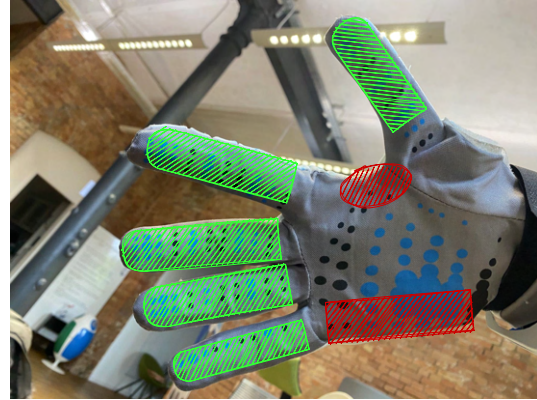
This result can be applied to Human-Robot Handshaking. It demonstrates that the grip force from the human hand acts mainly on the palm of the robot hand, while the grip force received by the human hand comes mainly from the fingers of the robot hand.

The BionicSoftHand wears a glove with tactile force sensors on fingers and palm, which allows it to sense the grip force when the object is gripped. So the human grip force F_H in handshaking can be measured by sensors on the palm of the BionicSoftHand. Moreover, the robot grip force F_R can be measured by sensors on the fingers of the BionicSoftHand, as shown in Figure 3.5 (a). A more intuitive representation is shown in Figure 3.5 (b).

The red area shows the contact area between the human hand and the BionicSoftHand's palm, and the green area shows the contact area between the BionicSoftHand's fingers and the human hand.



(a) Gripping force in Human-Robot Handshaking



(b) Contact area between the human hand and the BionicSoftHand

Figure 3.5.: The gripping force and contact area representation in Human-Robot Handshaking. While handshaking, human applies on the palm of the BionicSoftHand (the red area) a force F_H , while the fingers of the BionicSoftHand (the green area) apply a force F_R to the human hand.

3.3. Proposed Methods

This section proposes a control model for Human-Robot Handshaking, namely the Force-Impedance control. It combines the admittance control and the PID control to control the grip force and motion of the BionicSoftHand while Human-Robot Handshaking, where the PID controller will be used to control the robot grip force and the admittance controller be used to control the motion of the BionicSoftHand.

A spring system can model the handshake interaction between the human hand and the BionicSoftHand. We do the Force-Impedance control for this system. In Section 3.1.1, we have given the impedance and admittance models. We want the robot hand to adjust its motion according to the grip force, so we use the admittance control with

force command as input and motion command as output. According to Equation 3.6, the following admittance model is given,

$$K e_q = F_R, \quad (3.13)$$

where K is the stiffness, a control parameter, e_q is the position difference, F_R is the grip force exerted by the BionicSoftHand.

Equation 3.13 is similar to a P controller, which imposes a spring behavior on the mechanism by maintaining a dynamic relationship between force and position, where K is the control parameter. The dynamical properties of the BionicSoftHand are changed by adjusting K .

We aim to control the force exerted to the human hand, F_R , to guarantee the grasp's stability and not break components. Therefore a force controller is necessary. Generally, PID control can be used as the force control. Thus, we propose a method, namely the Force-Impedance control method, which combines the PID control and admittance control. By this model, the BionicSoftHand can adjust its grip force, F_R , to implement comfortable Human-Robot Handshaking.

The handshake model is shown in Figure 3.6. We use the PID controller to control the robot gripping force, whose setpoint is $F_{desired}$. The result of the PID controller will be used as input for the admittance control. The final generated command e_q controls the motion of the BionicSoftHand.

If we use the human grip force as the reference force, the handshake process can be summarised.

- The human hand comes into contact with the BionicSoftHand and grips its palm, the sensors on the palm detect the human gripping force F_H .
- The PID controller uses the human gripping force as the reference force $F_{desired}$. It calculates the difference e_F between the reference force $F_{desired}$ and the gripping force of the BionicSoftHand F_R (When the BionicSoftHand is fully open, its gripping force is 0, i.e., $F_R = 0$.), and it controls F_R to approach $F_{desired}$ gradually. Additionally, We obtain the intermediate control output of the PID controller u .
- In the admittance control, u is an input command, and the output is e_q , which will be used to move the BionicSoftHand.
- When the BionicSoftHand is closing, it contacts the human hand, and the sensors on the fingers detect F_R .

- F_R is used as feedback to compare with $F_{desired}$ to update the control command. In this case, the BionicSoftHand continues to adjust its grip force according to the reference force.

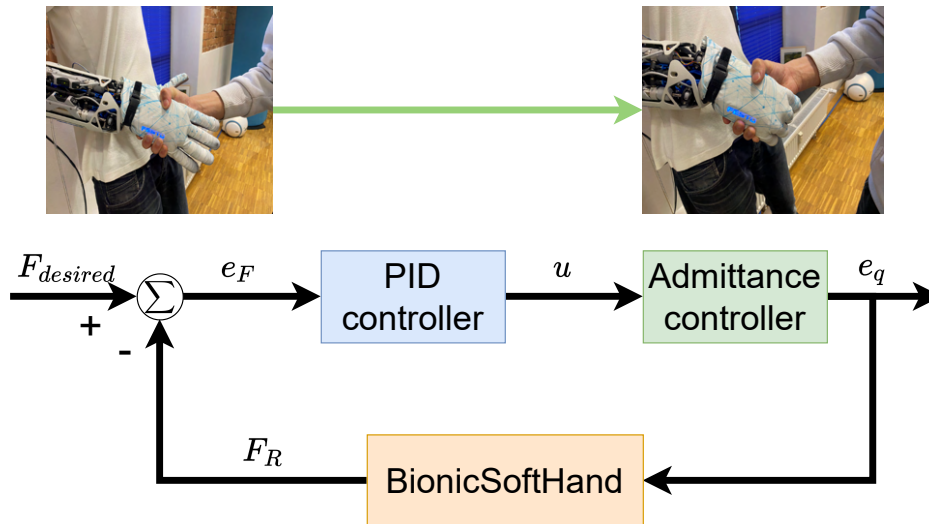


Figure 3.6.: Force-Impedance control for Human-Robot Handshaking. $F_{desired}$ presents the reference force for the force controller. F_R presents the robot grip force measured by sensors on the BionicSoftHand. e_F presents difference between $F_{desired}$ and F_R . u shows a command from the result of the force controller. e_q is a command that controls the motion of the BionicSoftHand.

In our control model, we need to determine the control parameters of the PID controller and the parameters of the admittance control. We hope the BionicSoftHand gives a comfortable handshake by suitable parameter tuning. A Handshake is an interactive behavior, if the human grip force is used as the reference force, the robot hand will continuously adjust its grip according to the human grip. With our control model, we hope that the robot hand imitates the human grip to give a pleasant handshake and more human-likeness in Human-Robot Handshaking.

4. Experiments and Results

This chapter presents our experiments about Human-Robot Handshaking. Section 4.1 describes the experimental setups, including the hardware setup and the software setup. In Section 4.2, we implement the human grip force and robot grip force calibration in Human-Robot Handshaking. Section 4.3 proposes an essential Human-Robot Handshaking interaction that does not involve the control for the robot grip force based on [8]. In Section 4.4, we introduce an improved Human-Robot Handshaking interaction based on the Force-Impedance control, where the PID controller as the force controller is considered to control the robot gripping force. Finally, we derive the experimental results and evaluate the results.

4.1. Experiment Setups

In this section, we describe the experimental setups. First, in subsection 4.1.1, We give a detailed introduction of the Festo BionicSoftHand 2.0 [29] [30], and most notable are the sensors and degrees of freedom of the hand. The sensors enable the measurement of grip force, while the degrees of freedom are for the hand's flexible opening and closing. Then, in subsection 4.1.2, we present the software setup of the experiment, which describes how we implement the communication with the hand and the motion control of the hand.

4.1.1. Hardware Setup

The Festo BionicSoftHand 2.0 [29] [30], shown in Figure 4.1, is a pneumatically controlled robot hand. It controls its movements via the pneumatic bellows structures in its fingers. There are 24 valves inside the hand, including 12 supply valves and 12 exhaust valves. When the chambers are filled with air, the fingers bend. If the air chambers are empty, the fingers remain stretched. Moreover, the thumb and index finger are also equipped

with swivel modules, which allow these two fingers to be moved laterally. In addition, a sensor glove with force sensors that cover the palm and fingers covers the hand, allowing sensing the magnitude and location of forces exerted on the hand. covers the hand



Figure 4.1.: Festo BionicSoftHand 2.0 [29] [30]. A sensor glove with force sensors that cover the palm and fingers covers the hand, allowing sensing the magnitude and location of forces exerted on the hand. The fingers are covered in a firm yet yielding knitted fabric, making it flexible to control and giving it a soft feel when touched. A compact valve terminal with 24 proportional piezo valves is used for precisely ventilating and exhausting fingers and controlling the motion modules.

The Festo BionicSoftHand 2.0 has twelve degrees of freedom, as shown in Table 4.1. Each degree has a corresponding actor to control the hand motion.

Index	Controlled degree of freedom	Description
0	Thumb side	Rotate the thumb left or right
1	Thumb lower	Open or close the lower part of the thumb
2	Counter pressure	The counter pressure is used for the wrist cylinders, the index side and the thumb rotation as restoring spring
3	Thumb upper	Open or close the upper part of the thumb
4	Index finger upper	Open or close the upper part of the index finger
5	Wrist left	Move the left wrist cylinder up or down
6	Index finger lower	Open or close the lower part of the index finger
8	Wrist right	Move the right wrist cylinder up or down
9	Index side	Move the index finger left or right
10	Ring finger	Open or close the ring finger
11	Pinky	Open or close the pinky

Table 4.1.: Degrees of freedom of the Festo BionicSoftHand 2.0¹. There are 12 degrees of freedom, with each index has a corresponding actor.

4.1.2. Software Setup

To interact with the BionicSoftHand, we first need to establish essential communication. The BionicSoftHand communicates with its python libraries via Ethernet. These python libraries provide a primary interface to communicate with the hand. To integrate it more into the robotic world, a ROS [31] interface implementation is provided. Figure 4.2 shows a basic software architecture of the communication.

¹<https://github.com/Festo-se>

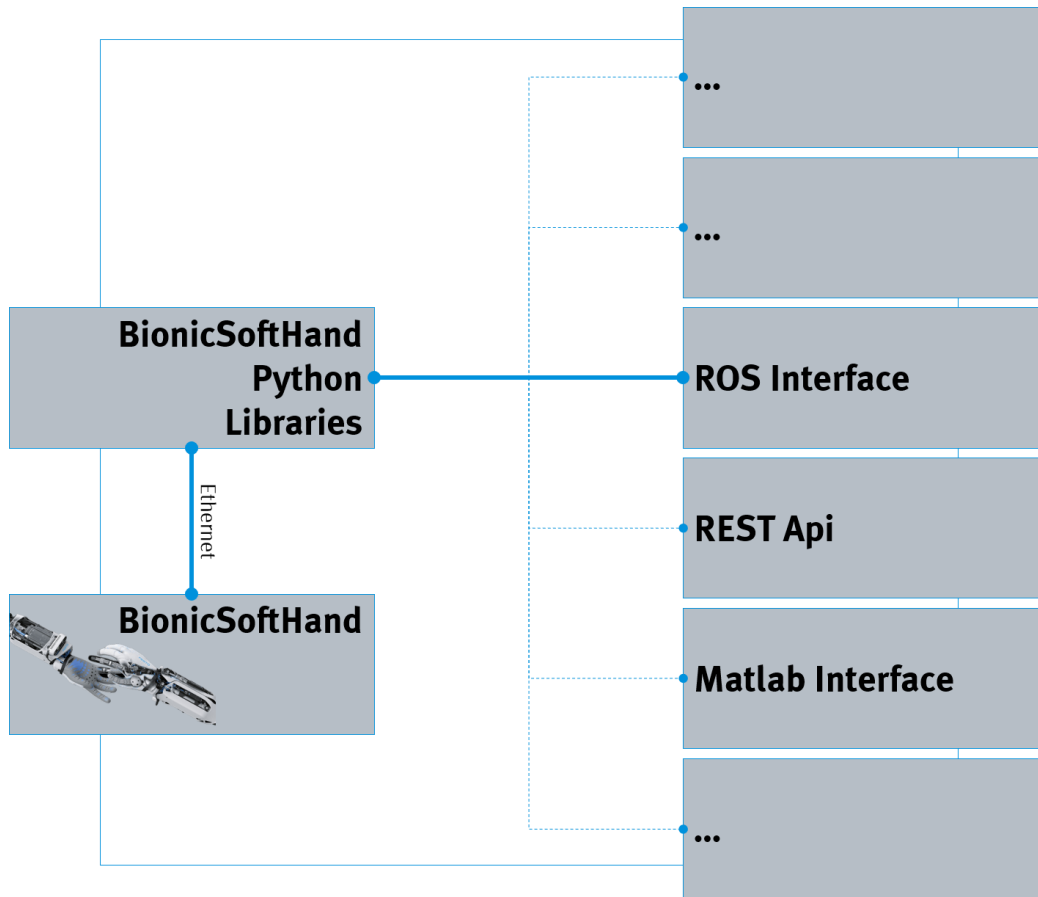


Figure 4.2.: Software architecture of the BionicSoftHand¹. The BionicSoftHand communicates with its python libraries via Ethernet. A ROS [31] interface implementation is provided with these python libraries.

If we want to mount the BionicSoftHand, we need a 24V or 48V power supply. Moreover, we also need to give an air supply to control it pneumatically. We should connect the exhaust tube and supply tube to the two tube connectors on the bottom side of the hand and notice that not more than 5 bars were given for safety. Next, connect the ethernet cable with our local network, which should be made sure in the same subnet with the IP address of the BionicSoftHand. Finally, we check for connection by executing a python

¹<https://github.com/Festo-se>

script in the python libraries, telling us if the hand is connected successfully.

If we successfully connect to the BionicSoftHand, we can implement simple control. We have a Graphical User Interface (GUI), as shown in Figure 4.4, with 12 sliders that correspond to the degrees of freedom in Table 4.1. We can control the robot's motion by manually sliding the sliders (from 0.0 to 5.0). Figure 4.3 shows a hand state by this simple control. This simple control is done manually, not involving interaction between a human and a robot.



Figure 4.3.: Simple control by the GUI. The BionicSoftHand grips the human hand by controlling all fingers to move with the sliders in the GUI.

HAND UI v1.5

| CONNECTED | AIR SUPPLY: 6.55 |

CONTROL MODE

VALVE | **PRESSURE** | WRIST | FINGER | POSITION

GRIP MODE

CUSTOM | CONCENTRIC | PARALLEL | CLAW

FINGERS

SPEED



OPEN | CLOSE

(0) THUMB SIDE	0(0.00)	<input type="range"/>	0(0.00)	<input type="range"/>
(1) THUMB LOWER	0(0.00)	<input type="range"/>	0(0.00)	<input type="range"/>
(3) THUMB UPPER	0(0.00)	<input type="range"/>	0(0.00)	<input type="range"/>
(9) INDEX SIDE	0(0.00)	<input type="range"/>	0(0.00)	<input type="range"/>
(6) INDEX LOWER	0(0.01)	<input type="range"/>	0(0.01)	<input type="range"/>
(4) INDEX UPPER	0(0.00)	<input type="range"/>	0(0.00)	<input type="range"/>
(8) MIDDLE FINGER	0(0.00)	<input type="range"/>	0(0.00)	<input type="range"/>
(10) RING FINGER	0(0.00)	<input type="range"/>	0(0.00)	<input type="range"/>
(11) PINKY	0(0.00)	<input type="range"/>	0(0.00)	<input type="range"/>
(2) COUNTER	0(0.01)	<input type="range"/>	0(0.01)	<input type="range"/>

WRIST

(5) LEFT	0(0.00)	<input type="range"/>	0(0.00)	<input type="range"/>
(7) RIGHT	0(0.00)	<input type="range"/>	0(0.00)	<input type="range"/>

Figure 4.4.: GUI for the motion control. When communication is successful, it will display the value of Air supply. We can then control the hand motion by sliding the 12 sliders corresponding to Table 4.1.

4.2. Force Sensing Grid Calibration

In this section, we point out an initial error in the grip force sensing for the BionicSoftHand. Then, we propose a method to reduce this error. Moreover, two experiments are done to calibrate the human grip force and the robot grip force.

From Section 3.2, we knew that sensors on the BionicSoftHand can measure the grip force. When no handshake occurs, a grid for visualizing the force is shown in Figure 4.5. Ideally, all the values in this grid should be 0 when no handshake occurs as no force can be detected. However, this is not the case. Therefore, there is some initial errors. Reducing these initial errors is essential for our experiments. We take the average of the first 100 measurements as an offset. Then we determine the result of subtracting this offset from the measured value as the actual measured value. Figure 4.6 shows the initial force-sensing grid after rectification. No exceptionally high values occur in the grid after rectification.

After the error rectification, we can then use the values in the grid to calculate the grip force. Thus, we need to determine which values in the grid can represent the force applied on the hand palm and can be used to calculate the human grip force F_H , and which values in the grid can be used to calculate the robot grip force F_R . To solve this problem, we have carried out two small experiments to extract the subset of sensors that match the corresponding regions shown in Section 3.2, representing the human and robot force.

In the first experiment, we repeatedly grip the BionicSoftHand with remaining it fixed, as shown in Figure 4.7 (a). At the same time, we observe how the values change in the grid. We then find the region where the values display significant change. These values will be used to calculate the human grip force F_H . In the second experiment, we follow the same steps with the human hand fixed to find the region with significantly changed values, as shown in Figure 4.7 (b). These values will be used to calculate the robot grip force F_R .

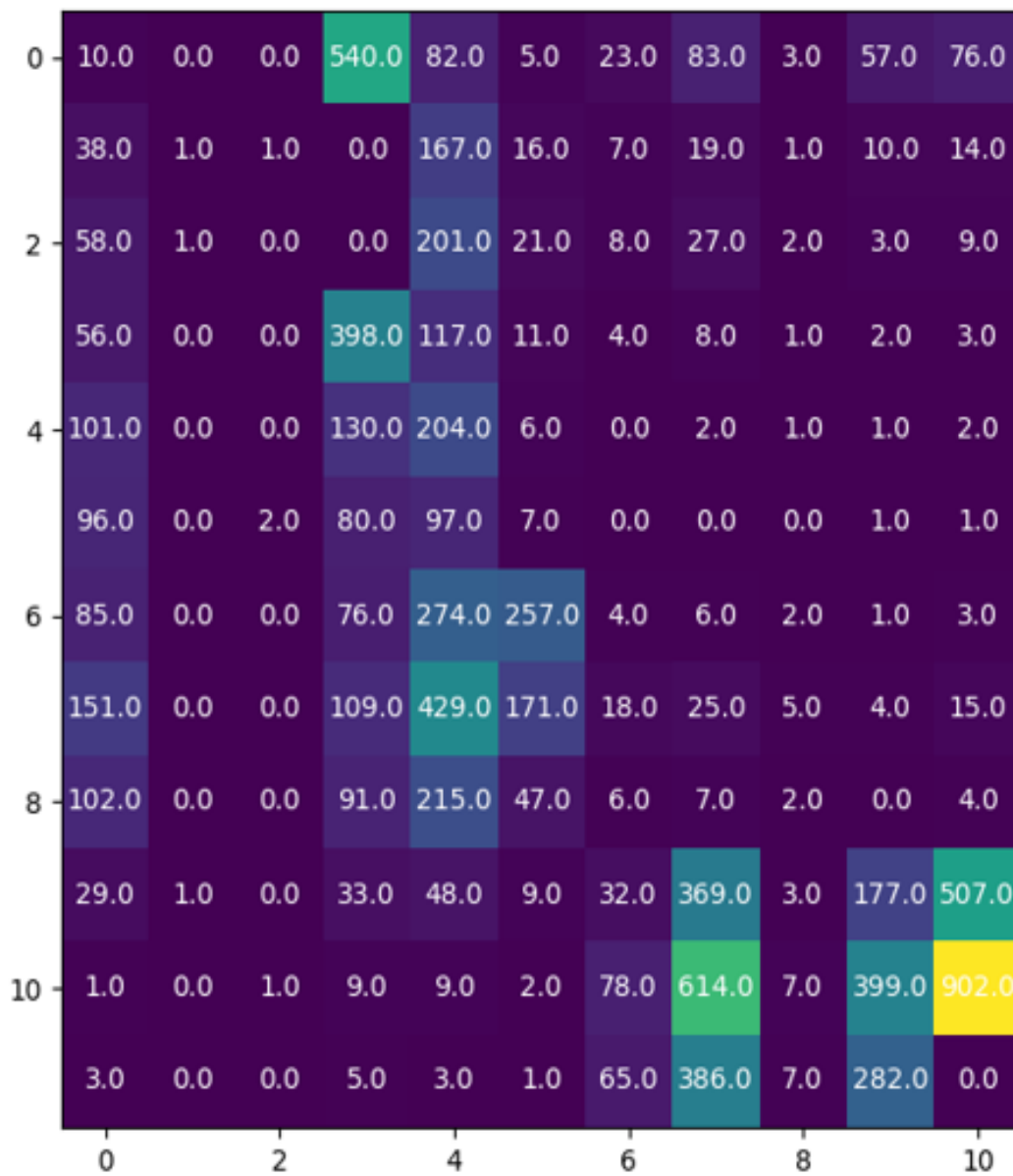


Figure 4.5.: Initial force-sensing grid. There are some high values, which indicates some initial errors in the force-sensing process. For example, the squeezing of the glove could cause these errors.

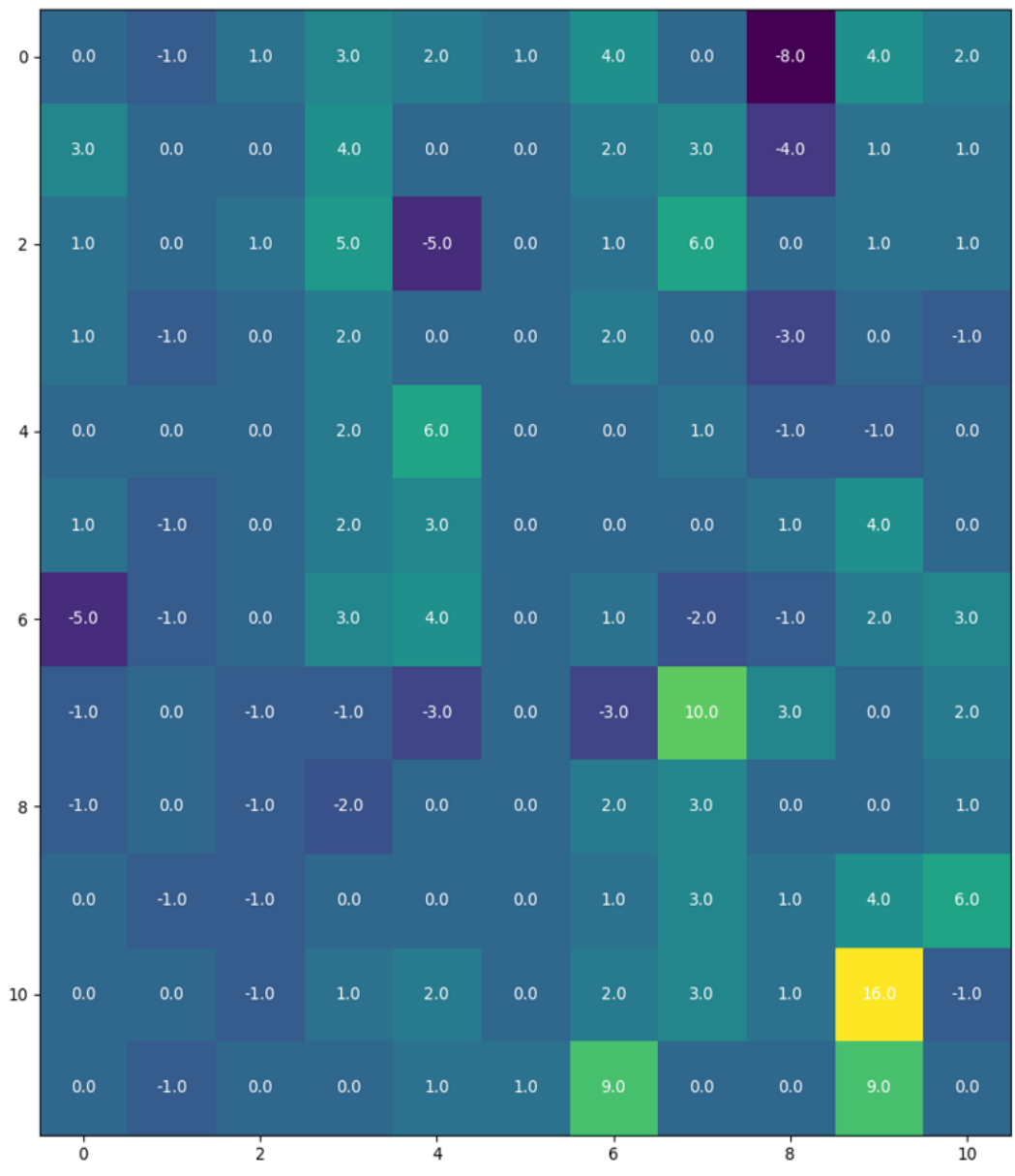


Figure 4.6.: Initial force-sensing grid after rectification. We obtain the result of subtracting an offset from the measured value as the actual measured value. There are no high values in the initial force-sensing grid after rectification.



(a) The human hand grips the BionicSoftHand



(b) The BionicSoftHand grips the human hand

Figure 4.7.: The region calibration experiments to calculate F_H and F_R . In (a), the human hand grips the BionicSoftHand. In (b), the BionicSoftHand grips the human hand. We observe how the values change in the grid while gripping in two experiments.

The results show that in both experiments, the values in the different regions of the grid change to different degrees. Based on these changes, we have calibrated two regions to calculate F_H and F_R respectively, as shown in Figure 4.7. We use colors and letters to represent the areas with significantly varying values.

The values in the red region A changed significantly in the first experiment, so it will be used to calculate F_H . The values in the grey region B changed significantly in the second experiment, so it will be used to calculate F_R . However, the values in the orange region C vary significantly in both experiments, indicating the measurement errors in this region. We, therefore, ignore the values in this region.

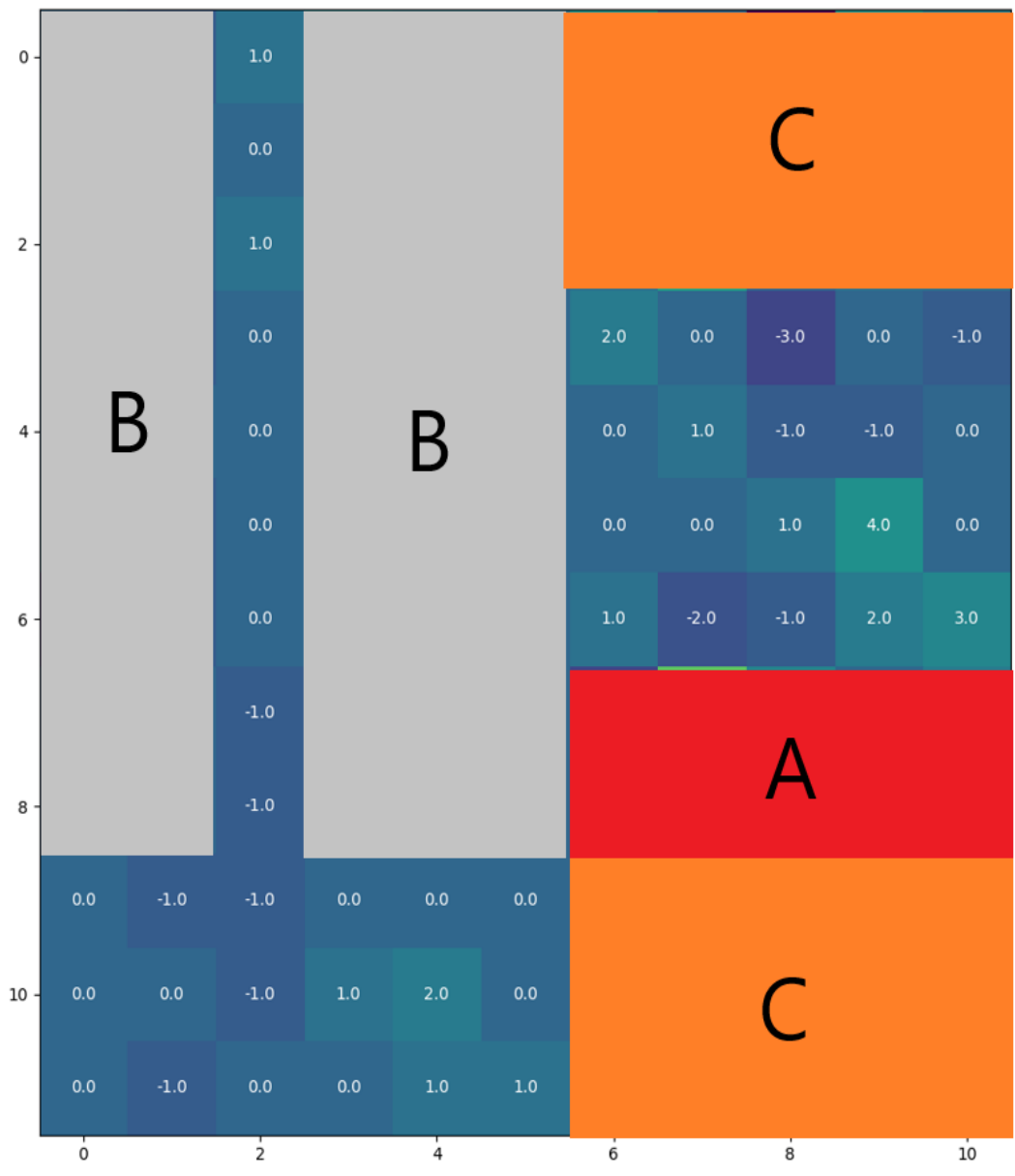


Figure 4.8.: Regions with significantly changed values. The values in the red region A changed significantly in the first experiment. The values in the grey region B changed significantly in the second experiment. The values in the orange region C vary significantly in both experiments.

4.3. Baseline Interactive Handshaking Behaviour

This section implements an essential Human-Robot Handshaking interaction, where no control for the robot grip force is implemented. Our approach is based on the work in [8]. The method was proposed to control the robot motion according to the human grip force.

Sensors on the BionicSoftHand can detect the human grip force, as seen in Section 3.2. In Section 4.2, we have calibrated the regions for calculating the human grip force F_H . We use the real-time measurement of the human grip force as the driving force for the motion of the BionicSoftHand, i.e., $e_q = KF_H$, e_q is the displacement command, K is the control parameter.

We set the control parameter K to $1/10$, $1/20$, and $1/30$ respectively to analyze the effect of parameters on the system dynamic and obtain the force curves of F_H and F_R shown in Figure 4.9 - 4.11.

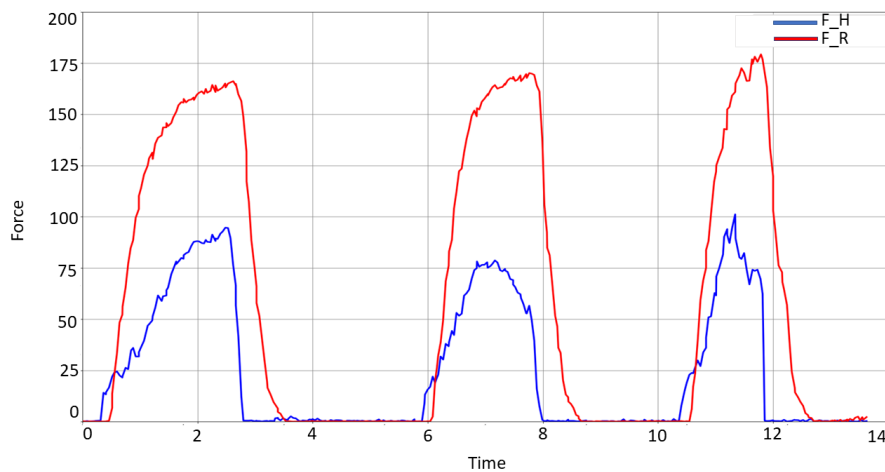


Figure 4.9.: The curve of the human grip force and the robot grip force for the parameter $K = 1/10$. The blue line presents the human grip force F_H , the red line presents the robot grip force F_R .

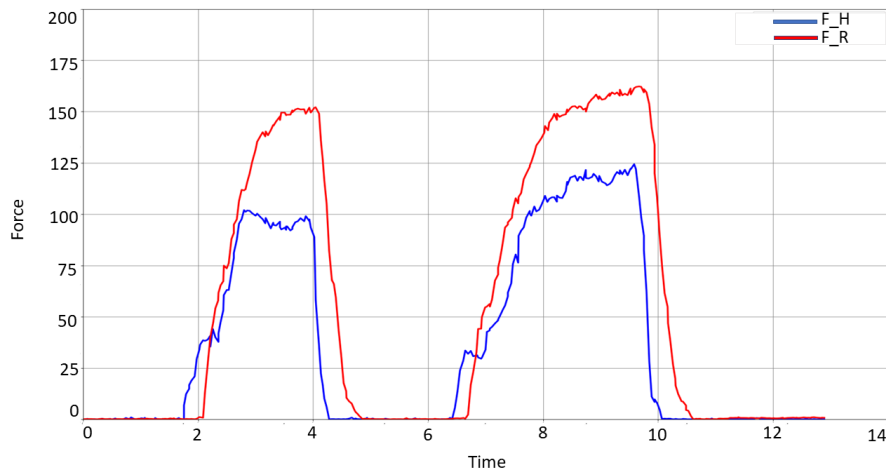


Figure 4.10.: The curve of the human grip force and the robot grip force for the parameter $K = 1/20$. The blue line presents the human grip force F_H , the red line presents the robot grip force F_R .

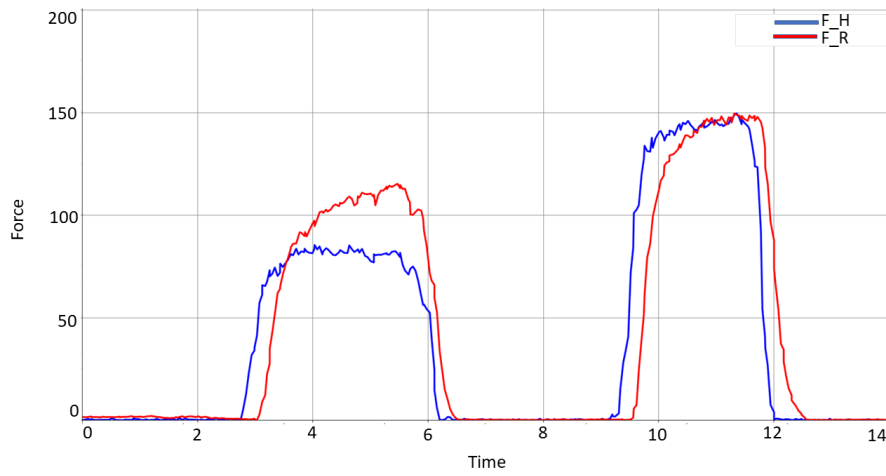


Figure 4.11.: The curve of the human grip force and the robot grip force for the parameter $K = 1/30$. The blue line presents the human grip force F_H , the red line presents the robot grip force F_R .

The result shows that a faster handshake response is felt by the human hand when $K = 1/10$ because, in this case, the rate of change of the control command is higher. Thus, for this control, a more considerable parameter value helps speed up the system's response and allows the BionicSoftHand to respond quickly to grip the human hand. As a result, the system's dynamic characteristics perform better in this case. However, the motion command e_q must be limited to a small range (from 0.0 to 5.0). A too fast response can also damage the the BionicSoftHand, as it is pneumatic, and its seal may be broken due to friction to affect its motion. Therefore, it is vital to choose the proper control parameters to control the BionicSoftHand to move within the control command range. The response speed should be improved in Human-Robot Handshaking, but the BionicSoftHand should be guaranteed not to be damaged.

In this interaction, the grip force of the robot hand is not controlled. As shown in Figures 4.9 and 4.10, it exceeds the grip force of the human hand by a lot, and the situation is slightly better in Figure 4.11. In the second peak, the grip force of the robot hand and the human hand can match. However, this case is very random. This result is almost identical to the one obtained by Vigni et al. [8], where also no control for the robot grip force was implemented. In this case, for different human hand sizes, the force that the robot exerts on the human hand may be also very different.

4.4. Improved interactive Handshaking Behavior

This section presents an improved Human-Robot Handshaking model, namely the Force-Impedance model. We use the PID controller to control the robot gripping force F_R and regard the human grip force F_H as the desired force. The output of the PID control as command input to the admittance control generates the control command e_q to control the motion of the BionicSoftHand. The Force-impedance control model implements the control for the robot grip force and the regulation for the motion of the BionicSoftHand.

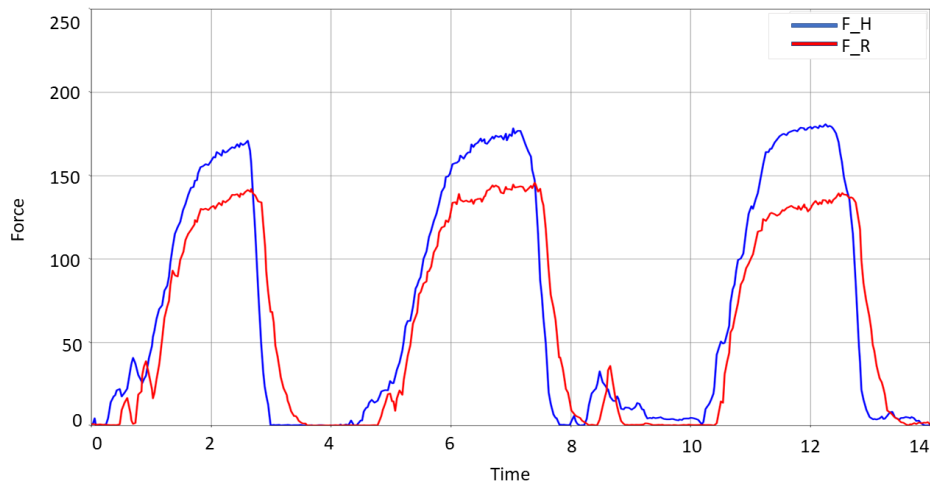
In our experiments, we obtained different Force-Impedance models by setting the different parameters of the Force-Impedance control. For the admittance control, we set the parameters $K = 1/30$ and $K = 1/40$. For the PID control, we compared three different controllers, i.e. P, PD, PID controller and the control parameters were set as $K_p = 2.4$, $K_i = 0.6$, $K_d = 1.2$. We evaluate the Force-Impedance models for different PID controllers and different admittance control parameters by visualizing the relationship curves between the human grip force F_H and the robot grip force F_R . Figures 4.12, 4.13, and 4.14 show

the relationship curves between F_H and F_R for the Force-Impedance control with P, PI, PID controller.

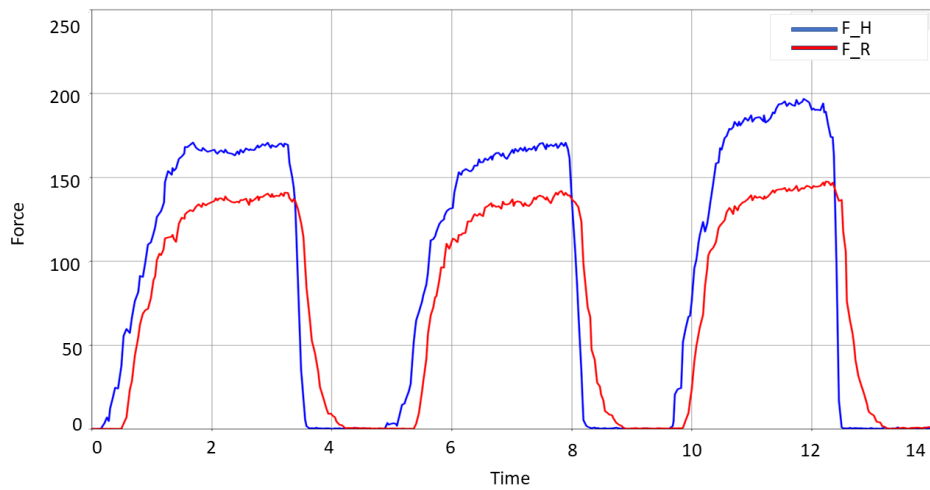
Furthermore, we are interested in how the magnitude of the PID control parameters affects the dynamics of the Force-Impedance model. We, therefore, update the parameters of the PID controller to obtain more relational curves between the human grip force F_H and the robot grip force F_R . For the Force-Impedance control model in Figure 4.14, we update respectively the PID control parameters K_p to 1.3 (Figures 4.15), K_d to 0.5 (Figures 4.16), K_i to 1.1 (Figures 4.17) and obtain the relationship curves between F_H and F_R .

The result shows:

- For the admittance control parameters, we obtain the same results as in Section 4.3, i.e., the more considerable the parameter, the faster the system response. For example, the model's response in Figure 4.12 (a) is faster than that of Figure 4.12 (b).
- For the different PID controllers, the PD controller improves the system's response compared to the P controller. However, this improvement is not very significant, such as when comparing Figure 4.13 (b) and 4.12 (b). Moreover, the PID controller reduces the steady-state error compared to the PD control and allows the BionicSoftHand to generate a grip force as close as possible to the human grip force. Nevertheless, reduces the system's response speed to a certain extent, such as when comparing Figure 4.14 (a) and 4.13 (a).
- For the different parameters of the PID controllers, the system responds slower as K_p decreases, such as when comparing Figure 4.15 (a) and 4.14 (a). The system's response also becomes slower as K_d decreases, such as when comparing Figure 4.16 (b) and 4.14 (b). The steady-state error reduces and the system responds slightly slower as K_i increases, such as when comparing Figure 4.17 (b) and 4.14 (b).

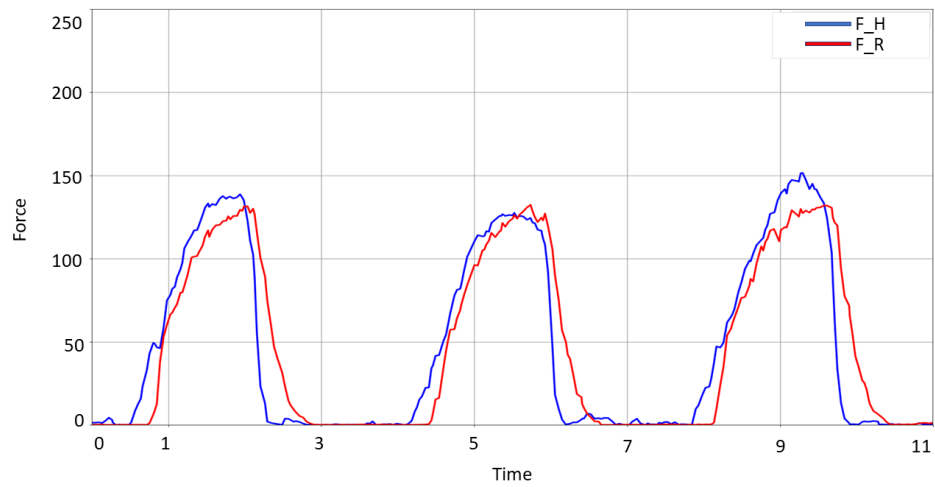


(a) Force-Impedance control with P controller for the admittance parameter $K = 1/30$

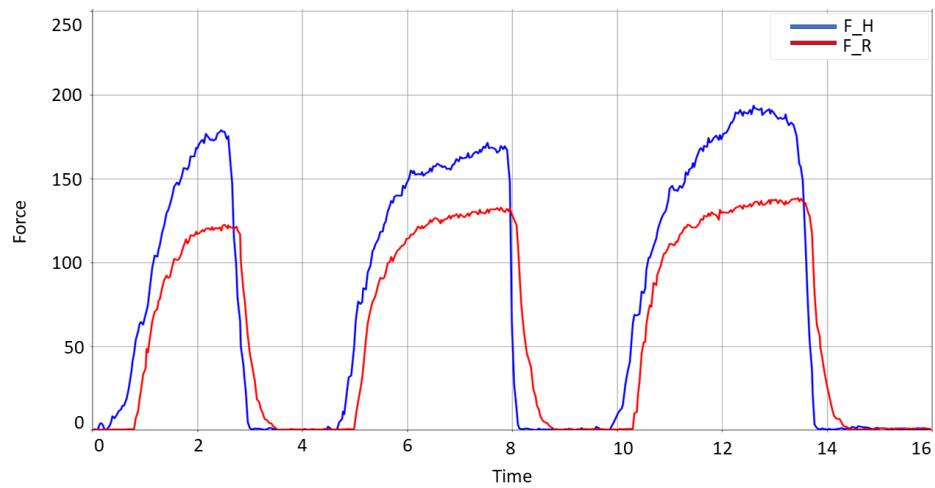


(b) Force-Impedance control with P controller for the admittance parameter $K = 1/40$

Figure 4.12.: The curve of the human grip force and the robot grip force with P controller for $K_p = 2.4$. The blue line presents the human grip force F_H , the red line presents the robot grip force F_R .

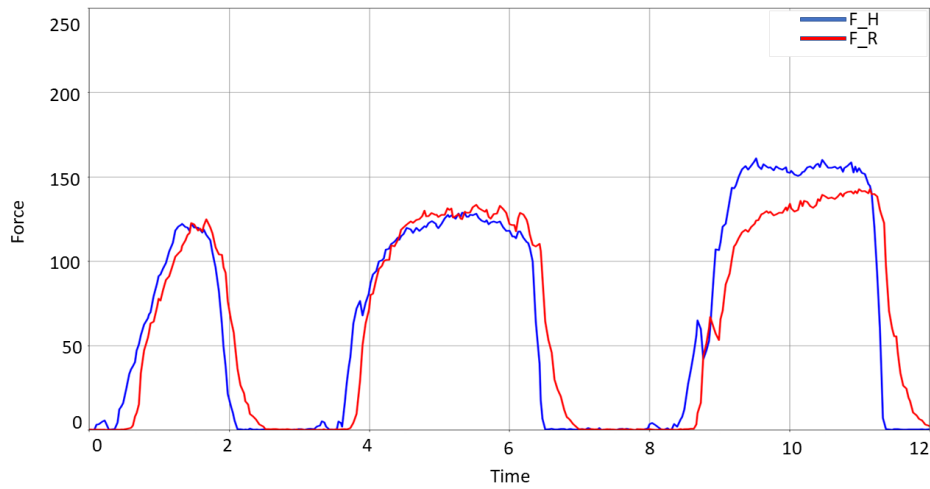


(a) Force-Impedance control with PD controller for the admittance parameter $K = 1/30$

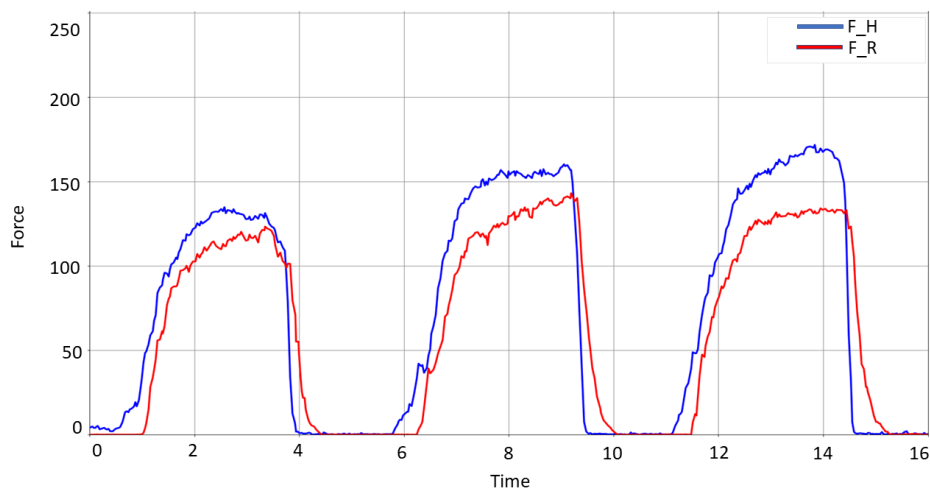


(b) Force-Impedance control with PD controller for the admittance parameter $K = 1/40$

Figure 4.13.: The curve of the human grip force and the robot grip force with PD controller for $K_p = 2.4$, $K_d = 1.2$. The blue line presents the human grip force F_H , the red line presents the robot grip force F_R .

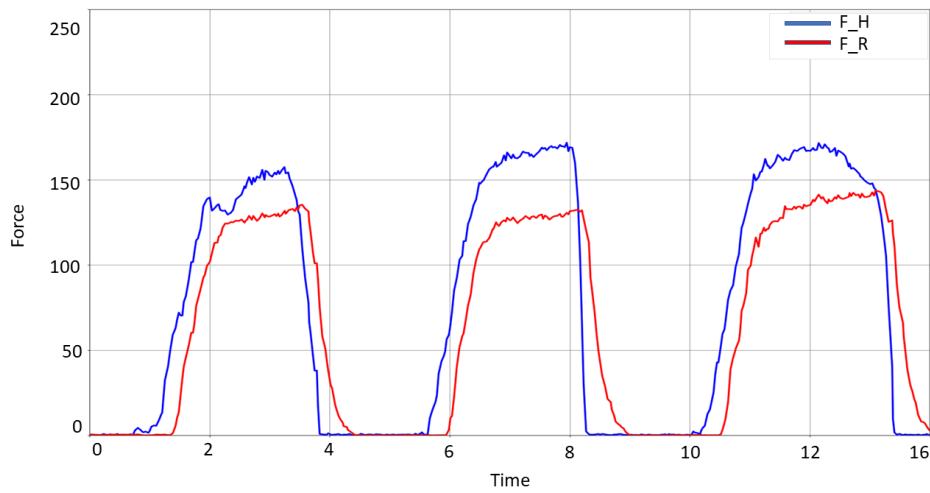


(a) Force-Impedance control with PID controller for the admittance parameter $K = 1/30$

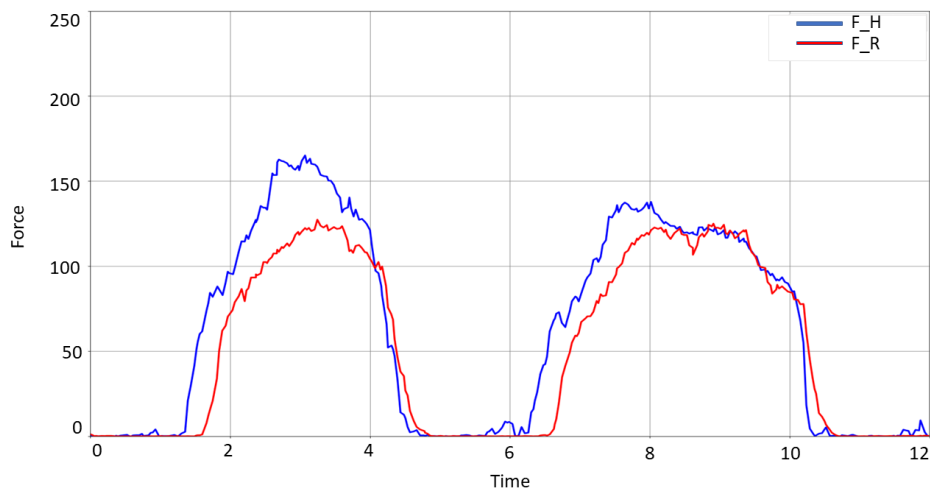


(b) Force-Impedance control with PID controller for the admittance parameter $K = 1/40$

Figure 4.14.: The curve of the human grip force and the robot grip force with PID controller for $K_p = 2.4$, $K_d = 1.2$, $K_i = 0.6$. The blue line presents the human grip force F_H , the red line presents the robot grip force F_R .

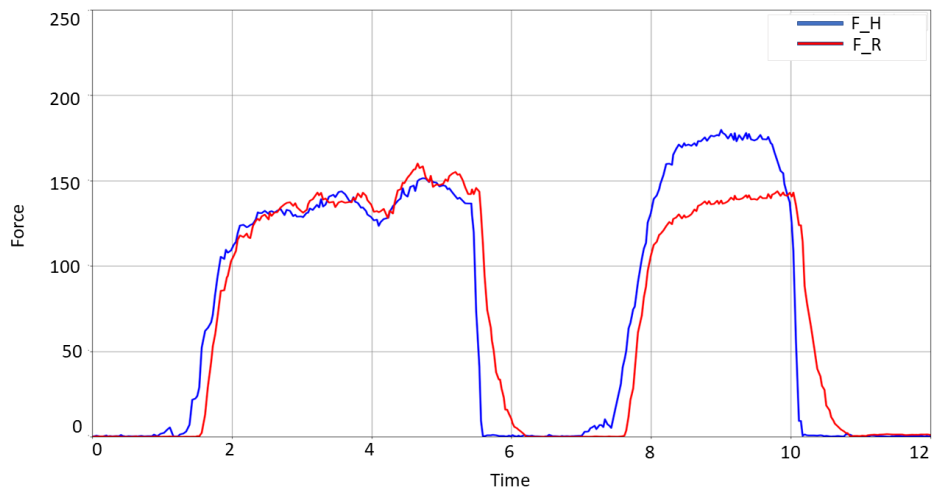


(a) Force-Impedance control with PID controller for the admittance parameter $K = 1/30$

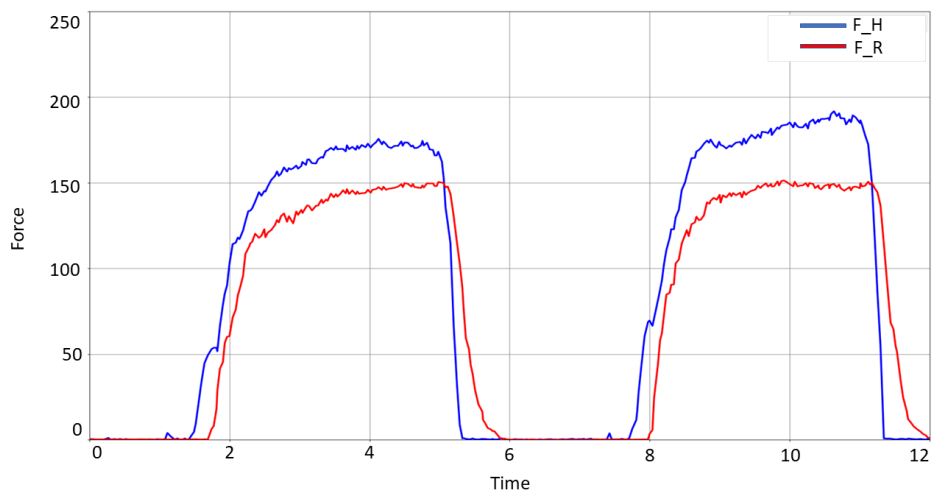


(b) Force-Impedance control with PID controller for the admittance parameter $K = 1/40$

Figure 4.15.: The curve of the human grip force and the robot grip force with PID controller for $K_p = 1.3$, $K_d = 1.2$, $K_i = 0.6$. The blue line presents the human grip force F_H , the red line presents the robot grip force F_R .

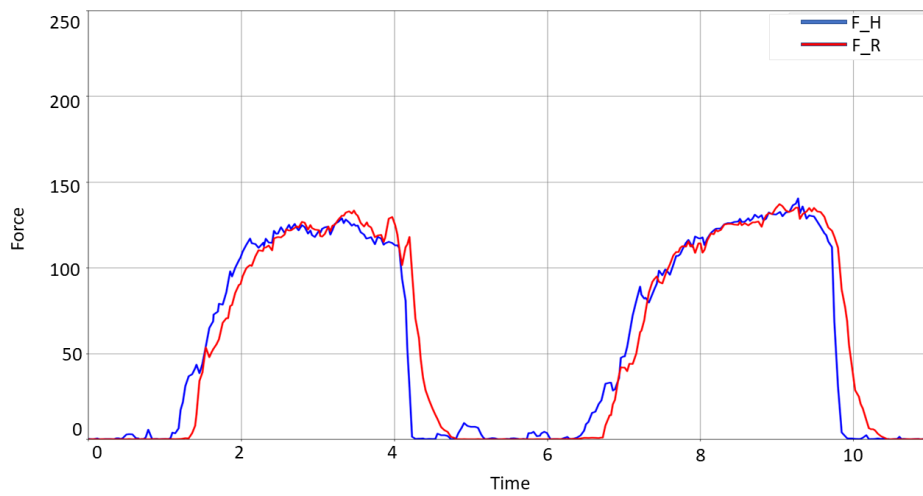


(a) Force-Impedance control with PID controller for the admittance parameter $K = 1/30$

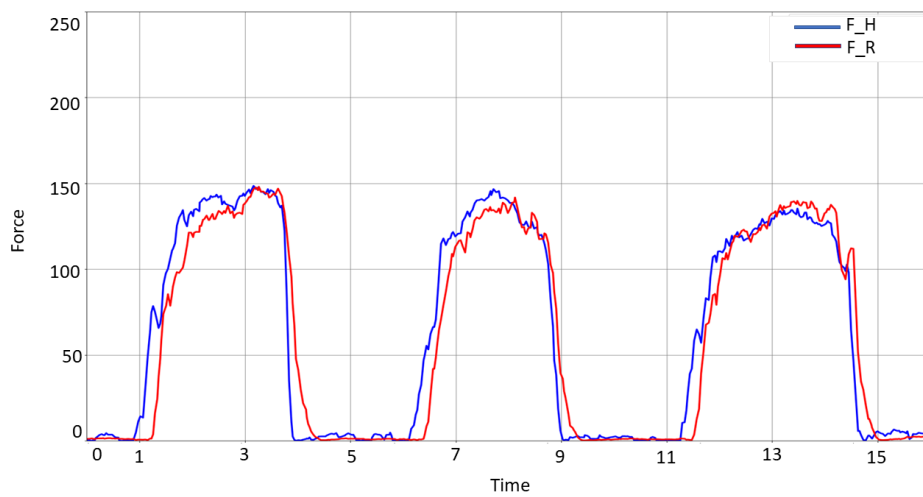


(b) Force-Impedance control with PID controller for the admittance parameter $K = 1/40$

Figure 4.16.: The curve of the human grip force and the robot grip force with PID controller for $K_p = 2.4$, $K_d = 0.5$, $K_i = 0.6$. The blue line presents the human grip force F_H , the red line presents the robot grip force F_R .



(a) Force-Impedance control with PID controller for the admittance parameter $K = 1/30$



(b) Force-Impedance control with PID controller for the admittance parameter $K = 1/40$

Figure 4.17.: The curve of the human grip force and the robot grip force with PID controller for $K_p = 2.4$, $K_d = 1.2$, $K_i = 1.1$. The blue line presents the human grip force F_H , the red line presents the robot grip force F_R .

The robot grip force plays an essential role in Human-Robot Handshaking. Too high a robot grip force can cause pain to the human hand and even hurt the human hand. On the other hand, too low grip force can lead to a loss of fun in Human-Robot Handshaking, as the human hand may not perceive the robot grip. Therefore, it seems that the parameters in Figure 4.17 are good choices. The resulting Force-Impedance model allows the robot grip force to be as close as possible to the human grip force while maintaining the responsiveness of the handshake interaction. In this case, the robot hand adjusts its grip force and motion according to the human grip. It allows for a comfortable and smooth Human-Robot Handshaking interaction.

A comfortable handshake is pleasurable and helps a robot interact better with a human. As a result, humans are more likely to interact with such a robot, which maximizes the capability of HRI. Such a robot could be used in many fields such as medicine and education without being disliked by humans.

5. Summary and Future Work

In this chapter, we summarise our work. Section 5.1 discusses our contributions and the shortcomings of our work. In Section 5.2, we then give an outlook on future work.

5.1. Summary

In this thesis, we proposed a control model, namely the Force-Impedance control, for Human-Robot Handshaking, which combines the PID control and admittance model, to explore the gripping behaviour and force of the BionicSoftHand in Human-Robot Handshaking. We extend the work of Vigni et al.[8], where they used the Pisa/IIT SoftHand [18], which can only measure the force exerted by the human hand, and the robot gripping force was estimated from the human grip force. Thus, the robot grip force can not be controlled in Human-Robot Handshaking. However, in our experiment, the robot gripping force F_R can be directly measured by the sensors on the fingers of the BionicSoftHand rather than be estimated. Therefore, we use our proposed model to control the robot gripping force and behaviour. As a result, the BionicSoftHand can better perceive the human gripping force and give a human hand a comfortable grasp.

In our model, the PID controller controls the BionicSoftHand to output an appropriate gripping force, while the admittance model controls the opening and closing of the BionicSoftHand. We cleverly combine these two components to form a closed-loop handshaking control. The results show that our control model can control the robot gripping force to approximate the human grip force. As a result, such a robot is more human-like. Furthermore, it further demonstrates the applicability of our control model and ensures a comfortable Human-Robot Handshaking.

However, our work also has a drawback. The sensor measurement errors of the BionicSoftHand is always present, even though we have reduced these errors as much as possible. As

a result, it impacts the accuracy of our experimental results. Fortunately, our control model is a generalized control model, which can control the robot gripping force to mimic the human grip force. Therefore, as long as the measurement errors are within an acceptable range, our results will not be significantly biased.

5.2. Future Work

In this thesis, we develop a handshake control model to explore the gripping behaviour and force of the BionicSoftHand in Human-Robot Handshaking. As a result, we can control the robot's handshake to show more human-like.

We can design a handshake experiment where we let a certain number of subjects shake hands with the BionicSoftHand. Then, we control the robot grip by the Force-Impedance model and design a questionnaire to investigate the subjects' perception of the robot grip in handshaking. Like the experiment in [8], we asked participants to perform a set of handshakes with the BionicSoftHand and then answer some questions as listed in Table 5.1, where answers are made on a 7-point Likert scale.

	Question	Scale (from 1 to 7)
Q1	Please rate the quality of the handshake	very poor to very good
Q2	Please rate the human-likeness of the handshake	very robot-like to very human-like
Q3	Please rate the responsiveness of the robot hand	not responsive at all to very responsive
Q4	How would you judge the personality of the robot hand	shy, hesitant, introvert, extrovert
Q5	Is the robot grip comfortable	not comfortable at all to very comfortable
Q6	what a feeling or emotion do the robot grip give you	nervousness, excitement, sadness, disappointment

Table 5.1.: Questions and answers about Human-Robot Handshaking [8]. We asked participants to perform a set of handshakes with the BionicSoftHand and then answer some questions, and answers were made on a 7-point Likert scale.

We record the feelings of the subjects and the corresponding robot grip force. According to the given questionnaire, we want the subjects to assess the quality of the handshaking, including the sensation of the grip and the grip strength. In addition, we would like to evaluate our model in comparison with the model in [8].

Furthermore, we would like to investigate further the haptic emotion detection based on the subjects' feedback. It is a valuable task, as some studies have shown that gripping force is related to haptic emotions.

Hertenstein et al. [32] [33] highlighted that humans could distinguish different emotions during the interpersonal touch on the arm and also on any body part (with stroke, tapping). The results showed that humans use touch to effectively communicate at least six different emotions (i.e., anger, fear, disgust, love, gratitude, and sympathy). In [23], it was also shown that it is possible to recognize gender and extroversion personality traits based on the firmness and movement of handshaking. For instance, smaller pressure and frequency were found to describe female handshakes, and higher speed amplitude describes introverted handshakes. Consistency was also found when comparing Human-Human Handshaking with Human-Robot Handshaking.

We propose future work about haptic emotion detection based on the above research. We can assume that humans with different emotions will show different grip strengths while handshaking. For example, a high grip strength represents emotions like nervousness and excitement, while a low grip strength may represent emotions like sadness and disappointment.

We collected the grip force data and emotion data from the user study and researched haptic emotion detection. On the one hand, we asked participants to evaluate the handshake. We hope the robot hand mimics the style of the human handshake and is more human-like to give a comfortable handshake. On the other hand, we hope that the robot hand can detect the gender or emotions based on the human grip behaviour and force in the handshaking.

Bibliography

- [1] M. Jindai, T. Watanabe, S. Shibata, and T. Yamamoto, "Development of a handshake robot system for embodied interaction with humans," in *ROMAN 2006 - The 15th IEEE International Symposium on Robot and Human Interactive Communication*, pp. 710–715, 2006.
- [2] D. Papageorgiou and Z. Doulgeri, "A kinematic controller for human-robot handshaking using internal motion adaptation," in *2015 IEEE International Conference on Robotics and Automation (ICRA)*, pp. 5622–5627, 2015.
- [3] M. Jindai, S. Ota, Y. Ikemoto, and T. Sasaki, "Handshake request motion model with an approaching human for a handshake robot system," in *2015 IEEE 7th International Conference on Cybernetics and Intelligent Systems (CIS) and IEEE Conference on Robotics, Automation and Mechatronics (RAM)*, pp. 265–270, 2015.
- [4] M. Hertenstein, J. Verkamp, A. Kerestes, and R. Holmes, "The communicative functions of touch in humans, nonhuman primates, and rats: A review and synthesis of the empirical research," *Genetic, social, and general psychology monographs*, vol. 132, pp. 5–94, 03 2006.
- [5] S. Yohanan and K. E. MacLean, "The role of affective touch in human-robot interaction: Human intent and expectations in touching the haptic creature," *International Journal of Social Robotics*, vol. 4, pp. 163–180, 2012.
- [6] R. Stock-Homburg, J. Peters, K. Schneider, V. Prasad, and L. Nukovic, "Evaluation of the handshake turing test for anthropomorphic robots," in *Companion of the 2020 ACM/IEEE international conference on human-robot interaction*, pp. 456–458, 2020.
- [7] V. Prasad, R. Stock-Homburg, and J. Peters, "Human-robot handshaking: A review," *International Journal of Social Robotics*, pp. 1–17, 2021.

-
-
- [8] F. Vigni, E. Knoop, D. Prattichizzo, and M. Malvezzi, “The role of closed-loop hand control in handshaking interactions,” *IEEE Robotics and Automation Letters*, vol. 4, no. 2, pp. 878–885, 2019.
- [9] V. Prasad, R. Stock-Homburg, and J. Peters, “Advances in human-robot handshaking,” in *International Conference on Social Robotics*, pp. 478–489, Springer, 2020.
- [10] G. Tagne, P. Hénaff, and N. Gregori, “Measurement and analysis of physical parameters of the handshake between two persons according to simple social contexts,” in *2016 IEEE/RSJ International Conference on Intelligent Robots and Systems (IROS)*, pp. 674–679, 2016.
- [11] A. Melnyk, P. Henaff, V. Khomenko, and V. Borysenko, “Sensor network architecture to measure characteristics of a handshake between humans,” in *2014 IEEE 34th International Scientific Conference on Electronics and Nanotechnology (ELNANO)*, pp. 264–268, 2014.
- [12] M. Jindai and T. Watanabe, “Development of a handshake robot system based on a handshake approaching motion model,” in *2007 IEEE/ASME international conference on advanced intelligent mechatronics*, pp. 1–6, 2007.
- [13] M. Jindai and T. Watanabe, “A handshake robot system based on a shake-motion leading model,” in *2008 IEEE/RSJ International Conference on Intelligent Robots and Systems*, pp. 3330–3335, 2008.
- [14] M. Jindai and T. Watanabe, “A small-size handshake robot system based on a handshake approaching motion model with a voice greeting,” in *2010 IEEE/ASME International Conference on Advanced Intelligent Mechatronics*, pp. 521–526, 2010.
- [15] M. Jindai, S. Ota, H. Yamauchi, and T. Watanabe, “A small-size handshake robot system for a generation of handshake approaching motion,” in *2012 IEEE International Conference on Cyber Technology in Automation, Control, and Intelligent Systems (CYBER)*, pp. 80–85, 2012.
- [16] E. Knoop, M. Bächer, V. Wall, R. Deimel, O. Brock, and P. Beardsley, “Handshakiness: Benchmarking for human-robot hand interactions,” in *2017 IEEE/RSJ International Conference on Intelligent Robots and Systems (IROS)*, pp. 4982–4989, 2017.
- [17] R. Deimel and O. Brock, “A novel type of compliant and underactuated robotic hand for dexterous grasping,” *The International Journal of Robotics Research*, vol. 35, no. 1-3, pp. 161–185, 2016.

-
-
- [18] M. G. Catalano, G. Grioli, A. Serio, E. Farnioli, C. Piazza, and A. Bicchi, "Adaptive synergies for a humanoid robot hand," in *2012 12th IEEE-RAS International Conference on Humanoid Robots (Humanoids 2012)*, pp. 7–14, 2012.
- [19] K. Ouchi and S. Hashimoto, "Handshake telephone system to communicate with voice and force," in *Proceedings 6th IEEE International Workshop on Robot and Human Communication. RO-MAN'97 SENDAI*, pp. 466–471, 1997.
- [20] N. Pedemonte, T. Laliberté, and C. Gosselin, "Design, Control, and Experimental Validation of a Handshaking Reactive Robotic Interface," *Journal of Mechanisms and Robotics*, vol. 8, 09 2015. 011020.
- [21] J. Avelino, T. Paulino, C. Cardoso, P. Moreno, and A. Bernardino, "Human-aware natural handshaking using tactile sensors for vizzy a social robot," in *Workshop on behavior adaptation, interaction and learning for assistive robotics at RO-MAN*, 2017.
- [22] Z. Wang, J. Yuan, and M. Buss, "Modelling of human haptic skill: a framework and preliminary results," *IFAC Proceedings Volumes*, vol. 41, no. 2, pp. 14761–14766, 2008. 17th IFAC World Congress.
- [23] P.-H. Orefice, M. Ammi, M. Hafez, and A. Tapus, "Let's handshake and i'll know who you are: Gender and personality discrimination in human-human and human-robot handshaking interaction," in *2016 IEEE-RAS 16th International Conference on Humanoid Robots (Humanoids)*, pp. 958–965, 2016.
- [24] J. Avelino, T. Paulino, C. Cardoso, P. Moreno, and A. Bernardino, "Human-aware natural handshaking using tactile sensors for vizzy , a social robot," 2017.
- [25] P. Moreno, R. Nunes, R. Figueiredo, R. Ferreira, A. Bernardino, J. Santos-Victor, R. Beira, L. Vargas, D. Aragao, and M. Araújo, *Vizzy: A Humanoid on Wheels for Assistive Robotics*, pp. 17–28. 12 2016.
- [26] J. Avelino, T. Paulino, C. Cardoso, R. Nunes, P. Moreno, and A. Bernardino, "Towards natural handshakes for social robots: human-aware hand grasps using tactile sensors," *Paladyn, Journal of Behavioral Robotics*, vol. 9, no. 1, pp. 221–234, 2018.
- [27] M. Griffin, "Whole-body vibration," in *Encyclopedia of Vibration* (S. Braun, ed.), pp. 1570–1578, Oxford: Elsevier, 2001.
- [28] N. Hogan, "Impedance control: An approach to manipulation," in *1984 American Control Conference*, pp. 304–313, 1984.

-
-
- [29] “Bionicmobileassistant.” https://www.festo.com/us/en/e/about-festo/research-and-development/bionic-learning-network/bionicmobileassistant-id_326923/.
- [30] “Mobile robot system meets bionicsofthand 2.0.” <https://press.festo.com/en/bionics-1/mobile-robot-system-meets-bionicsofthand-2-0>.
- [31] M. Quigley, K. Conley, B. Gerkey, J. Faust, T. Foote, J. Leibs, R. Wheeler, A. Y. Ng, *et al.*, “Ros: an open-source robot operating system,” in *ICRA workshop on open source software*, vol. 3, p. 5, Kobe, Japan, 2009.
- [32] M. J. Hertenstein, D. Keltner, B. App, B. A. Bulleit, and A. R. Jaskolka, “Touch communicates distinct emotions.,” *Emotion*, vol. 6 3, pp. 528–33, 2006.
- [33] M. J. Hertenstein, R. Holmes, M. E. McCullough, and D. Keltner, “The communication of emotion via touch.,” *Emotion*, vol. 9 4, pp. 566–73, 2009.

A. Appendix

A.1. Topic Connection

In this section, we introduce the ROS [31] communication mechanism, and we describe how the messages are transmitted in the handshaking control model.

Figure A.1 illustrates the basic topic connection model of the BionicSoftHand. First, to control the BionicSoftHand, we start the BionicSoftHand Node, which talks to the BionicSoftHand and publishes Sensor Value Data Messages on the Sensor value Topic. Then, to process the sensor value data, we start the Handshaking Node and subscribe to the Sensor value Topic. After subscription, the Handshaking Node begins receiving Sensor Value Data Messages to generate Pressure Data. Then, the Handshaking Node publishes Pressure Data Messages on the Pressure Topic. Finally, the BionicSoftHand Node subscribes to the Pressure Topic and talks to the BionicSoftHand to issue control movement commands. End here, the topic connection between the two nodes is complete.

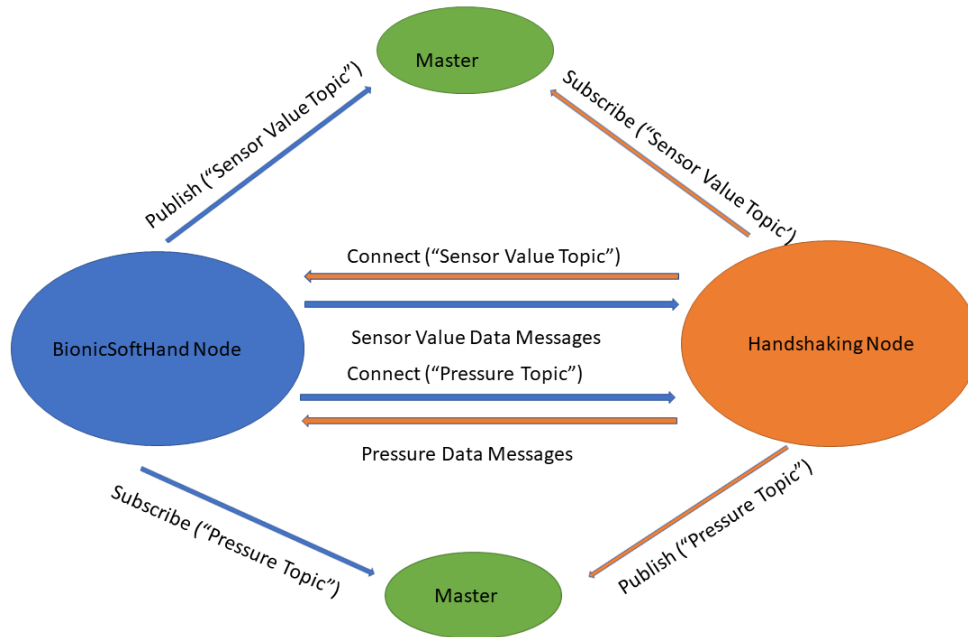


Figure A.1.: Topic connection model. It shows the transmission process of messages and the connection process between two ROS [31] nodes in handshaking.

A.2. Parameters Turning

In this section, we have made some adjustments to the parameters.

In Section 4.2, we calibrate the forces-sensing grid regions for the human grip force and the robot grip force by grip experiments. The result is shown in Figure 4.8, where we ignore the values in the orange region C. In this section, we take advantage of the values in C as well. Based on the distribution of sensors on the BionicSoftHand, the lower part of C belongs to the thumb, and the upper part of C belongs to the palm. Thus, for Figure 4.8, we recalibrate the regions for calculating F_H and F_R . We add region of the upper part of C to A, and add the region of the the lower part of C to B, as shown in Figure A.2. In order to utilize as many sensors as possible, we try to explore our experiments, although errors can be introduced.

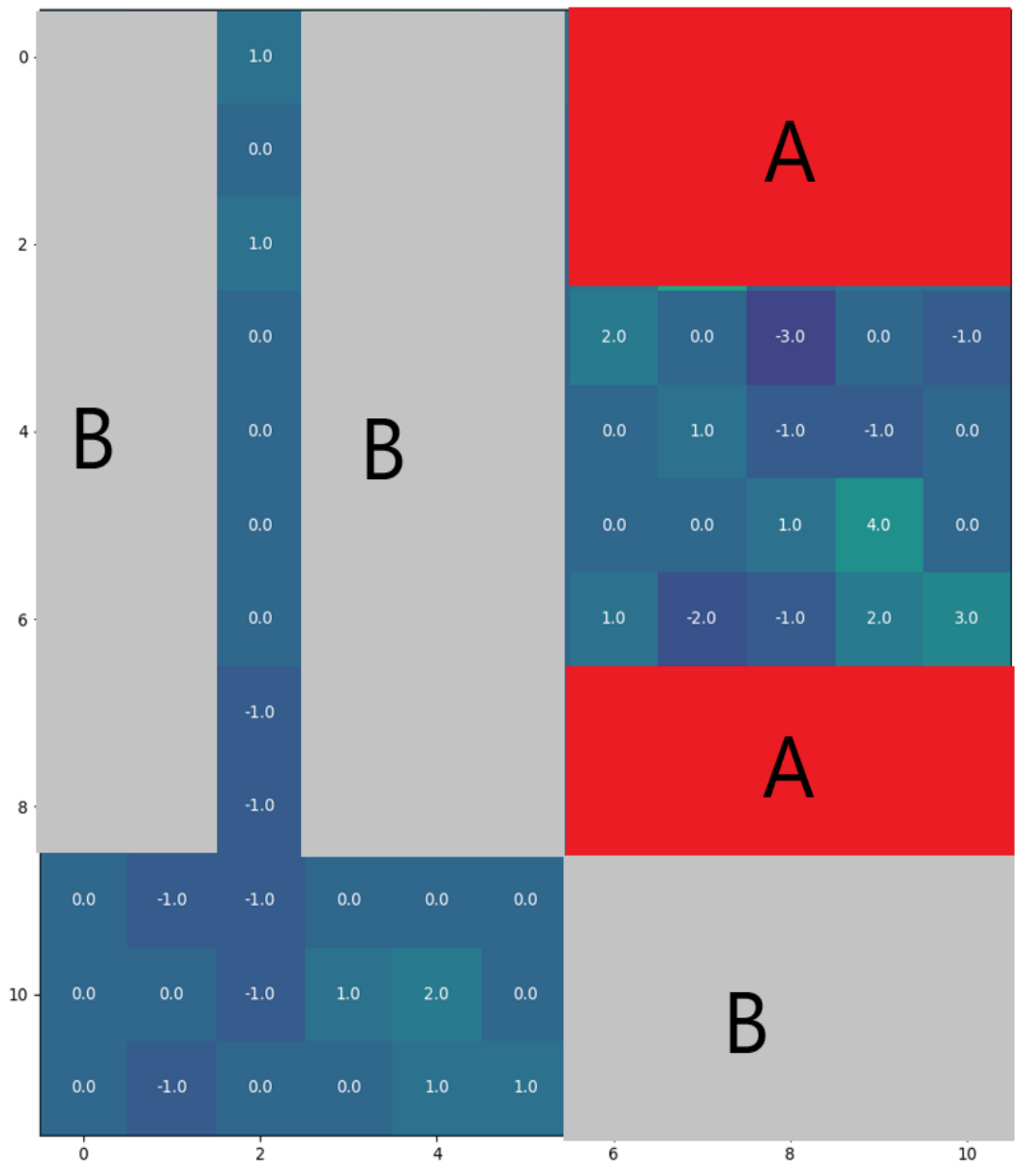


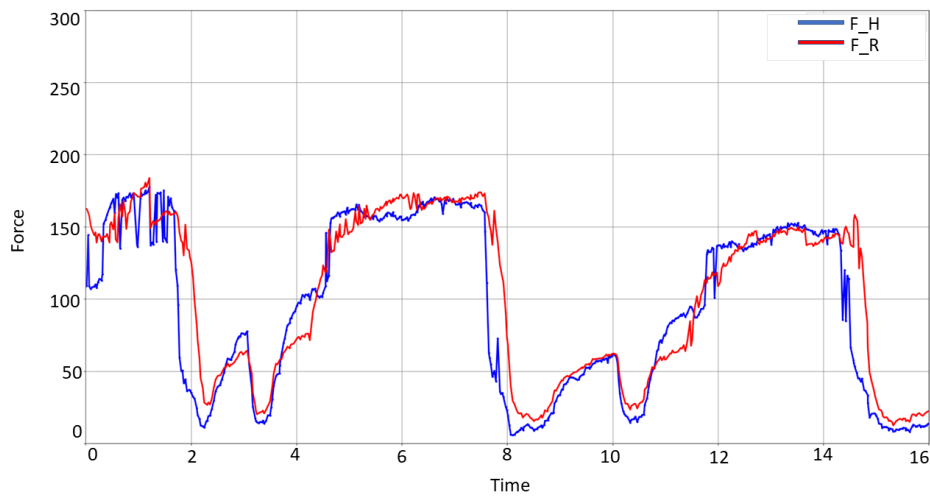
Figure A.2.: Regions with significantly changed values. The values in the red region A are used to calculate F_H . The values in the grey region B are used to calculate F_R .

In addition, for Section 4.4, we filter the control commands by using a multidimensional uniform filter to achieve a smooth effect for handshaking. Finally, we use the filtered commands to control the motion of the BionicSoftHand.

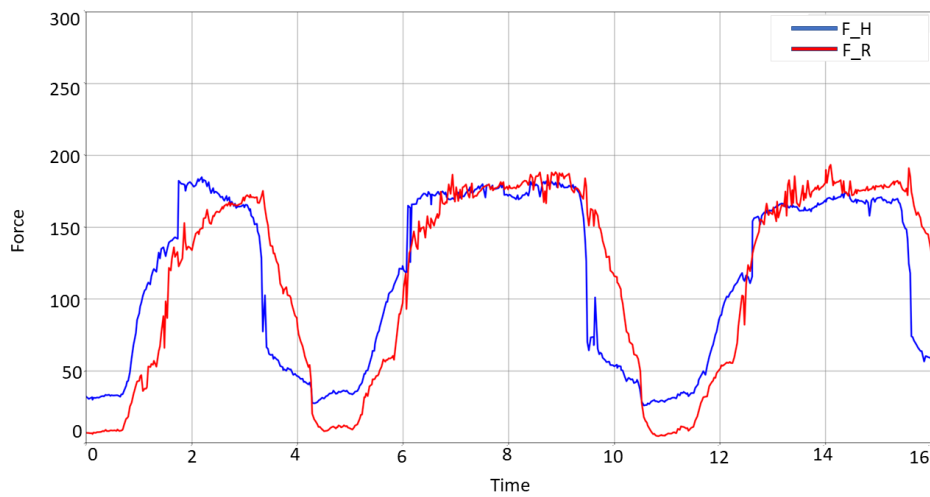
We adjust the PID controller parameters in the Force-Impedance model and compare the different controllers (P, PD, PI, PID controller). For the parameters of the admittance control, we do not adjust further, and we set $K = 1/40$. Figure A.3 - A.6 show the results.

From the results, it appears that the force fluctuates a lot. We guess that it is mainly due to the inclusion of adding the region C to A and B in the calibration of the human grip force and the robot grip force. It leads to possible significant errors in calculating the mean force value. Therefore, the system becomes unstable. In addition, the grip response of the robot hand is generally slower, which is speculated to be caused by the filter. Although the filter smoothed out the motion of the robot hand, it introduced some lag to the motion.

However, in general, the effect of the control parameters on the handshake model is consistent with the results we obtained in Section 4.4. Furthermore, because the PID controller controls a trend, the grip force of the robot hand will follow the grip force of the human hand even in the presence of errors.

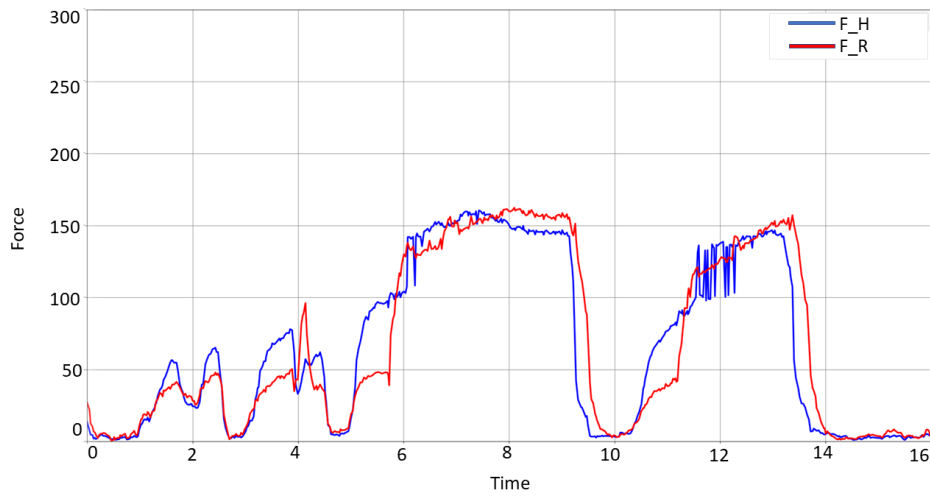


(a) Force-Impedance control with P controller for $K_p = 1.786$

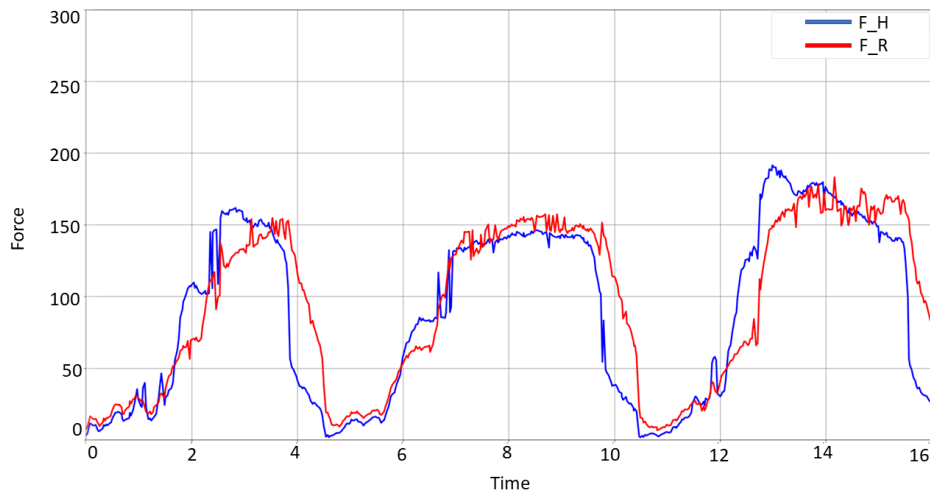


(b) Force-Impedance control with P controller for $K_p = 0.825$

Figure A.3.: The curve of the human grip force and the robot grip force with P controller. The blue line presents the human grip force F_H , the red line presents the robot grip force F_R . (a) shows that how F_H and F_R variate while handshaking for the Force-Impedance control parameter $K_p = 1.786$. (b) shows that how F_H and F_R variate while handshaking for the Force-Impedance control parameter $K_p = 0.825$.

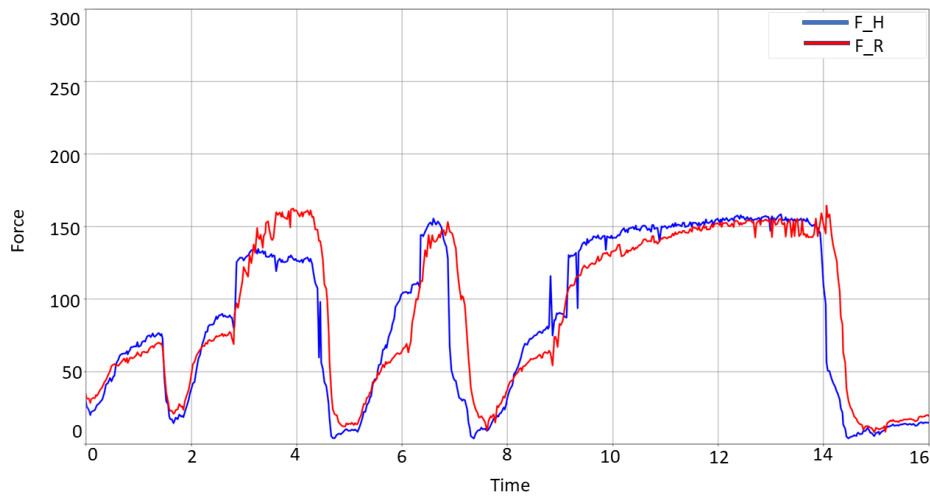


(a) Force-Impedance control with PD controller for $K_p = 1.786$, $K_d = 1.856$

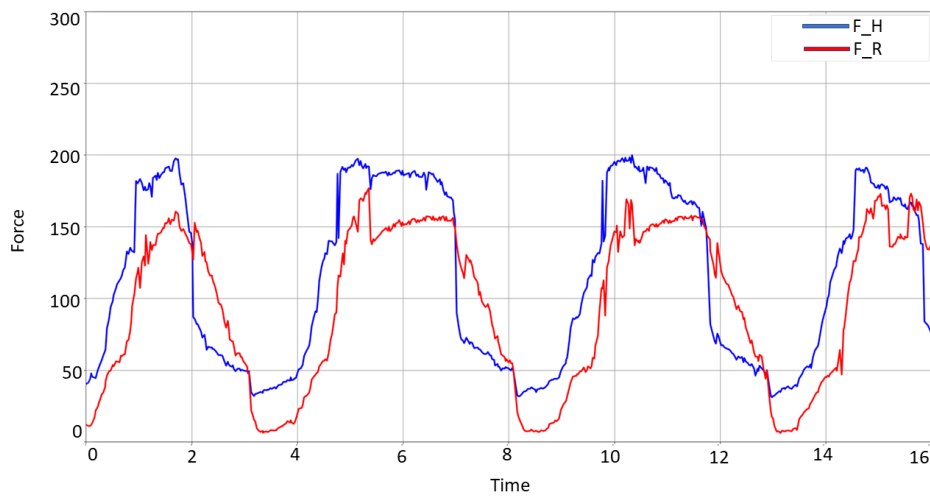


(b) Force-Impedance control with PD controller for $K_p = 0.825$, $K_d = 0.873$

Figure A.4.: The curve of the human grip force and the robot grip force with PD controller. The blue line presents the human grip force F_H , the red line presents the robot grip force F_R . (a) shows that how F_H and F_R variate while handshaking for the Force-Impedance control parameter $K_p = 1.786$, $K_d = 1.856$. (b) shows that how F_H and F_R variate while handshaking for the Force-Impedance control parameter $K_p = 0.825$, $K_d = 0.873$.

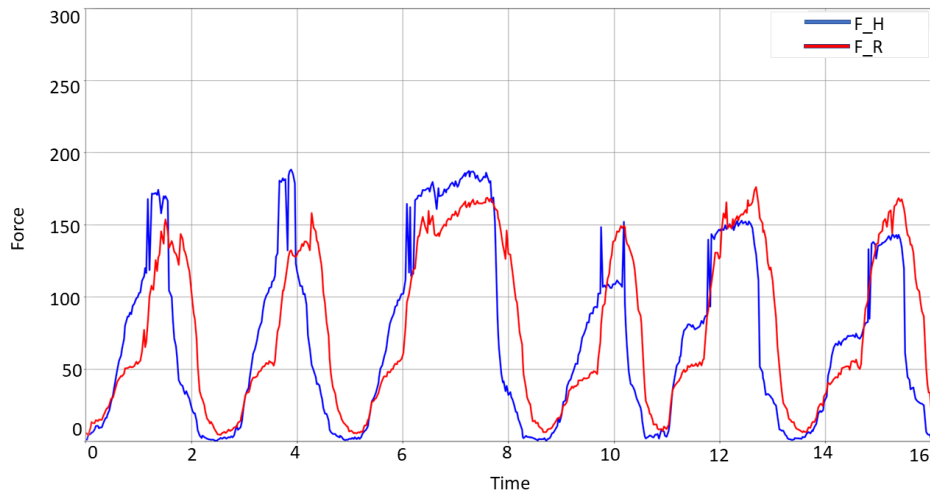


(a) Force-Impedance control with PI controller for $K_p = 1.786$, $K_i = 0.965$

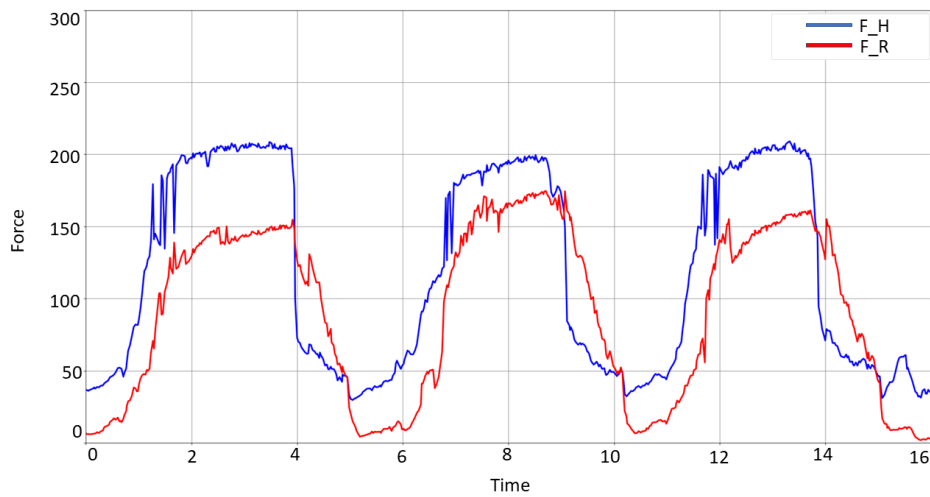


(b) Force-Impedance control with PI controller for $K_p = 0.825$, $K_i = 0.435$

Figure A.5.: The curve of the human grip force and the robot grip force with PI controller. The blue line presents the human grip force F_H , the red line presents the robot grip force F_R . (a) shows that how F_H and F_R variate while handshaking for the Force-Impedance control parameter $K_p = 1.786$, $K_i = 0.965$. (b) shows that how F_H and F_R variate while handshaking for the Force-Impedance control parameter $K_p = 0.825$, $K_i = 0.435$.



(a) Force-Impedance control with PID controller for $K_p = 1.786$, $K_i = 0.965$, $K_d = 1.856$



(b) Force-Impedance control with PID controller for $K_p = 0.825$, $K_i = 0.435$, $K_d = 0.873$

Figure A.6.: The curve of the human grip force and the robot grip force with PID controller. The blue line presents the human grip force F_H , the red line presents the robot grip force F_R . (a) shows that how F_H and F_R variate while handshaking for the Force-Impedance control parameter $K_p = 1.786$, $K_i = 0.965$, $K_d = 1.856$. (b) shows that how F_H and F_R variate while handshaking for the Force-Impedance control parameter $K_p = 0.825$, $K_i = 0.435$, $K_d = 0.873$.



Acknowledgments

We would like to thank Karoline von Häfen, Timo Schwarzer, Sebastian Schrof and Michael Jakob from Festo SE Co. KG for providing us with the BionicSoftHand 2.0 which has made this research possible. We would also like to thank Timo Schwarzer and Sebastian Schrof for all the technical support during the course of this research.